Vol. 2 December, 1957 No. 3

MINERALOGICAL JOURNAL

CONTENTS

A Spiral Weissenberg Apparatus for X-Ray Analysis ..... Y. Takano ... 143
Sericite from Ozawa-Mura, Gumma Prefecture... H. Kodama ... 151
X-Ray Surface Reflexion Fields on Precession Photographs..... Y. Takéuchi..... 162
Long Spacing Clay Mineral from the Uku Mine, Yamaguchi... Prefecture, Japan.....T. Mitsuda..... 169
A New Occurrence of Pyrosmalite in the Kyurazawa Mine, ... Tochigi Prefecture, Japan..... T. Watanabe and A. Kato..... 180
Short Communications
Diaspore Found in Association with Zincblende and Pyrite Ores of the Hanaoka Mine, Akita Prefecture .....T. Sudo and H. Hayashi... 187
Iron-rich Saponite from Mazé, Niigata Prefecture, Japan..... N. Miyamoto 193
Zeolit-Bearing Bentonite.....H. Hayashi and T. Sudo 196
Abstract of the Kobutsugaku Zasshi, Journal of the Mineralogical Society of Japan, Vol. 3, No. 3 200
Vol. 3, No. 4 204

The Mineralogical Society of Japan
Department of Geology and Mineralogy, Faculty of Science,
Hokkaido University, Sapporo, Japan

MINERALOGICAL JOURNAL

published by

The Mineralogical Society of Japan

EDITORIAL BOARD

Zyunpéi HARADA, *Hokkaido University;* Teiichi ITO, *University of Tokyo;* (Chief) Nobuo KATAYAMA, *University of Tokyo;* Keiichi OMORI, *Tohoku University;* Ryôiti KIRIYAMA, *University of Osaka;* Seitaro TSUBOI, *University of Tokyo;* Takeo WATANABE, *University of Tokyo;* Toyofumi YOSHIMURA, *Kyushu University.*

Instructions to Contributors

Manuscripts of articles should be submitted to the executive editor, Nobuo Katayama, at the College of General Education, University of Tokyo, Komaba, Meguro-ku, Tokyo. The manuscript should be type-written with double space lines, and not exceed 20 sheets of normal type-writing paper. References of literature should be in accordance with the forms used in the pages of this journal.

Plates and figures should be capable of reduction to not more than 10 by 15 centimetres. Line drawings should be in black India ink on white drawing board, tracing paper, or coordinate paper printed in blue. Photographs should be positive glossy prints.

Two referees chosen by the Editorial Board read the manuscript of article submitted before it is accepted for publication.

Thirty reprints without cover will be furnished to the author free of cost and without previous notice from him. Additional reprints will be furnished at cost when ordered.

The price of the journal to subscribers in Japan is 250 yen for a single copy (including postage), and to subscribers in other countries $ 1.00 (including postage) for a single copy, or $ 5.00 (including postage) per volume of 6 numbers.

Printed in Japan

MINERALOGICAL JOURNAL, VOL. 2, NO. 3, PP. 143-150, DEC., 1957

A SPIRAL WEISSENBERG APPARATUS FOR X-RAY ANALYSIS

YUKIO TAKANO

Institute of Earth Science, College of General Education, University of Tokyo

ABSTRACT

A new method of recording several layers of the reciprocal lattice simultaneously on a single photograph is proposed.

The method is a modification of the Weissenberg method with the film moving spirally on the surface of a cylindrical screen with several slits. The geometry of the diffraction patterns recorded by this method is, in general, different from those of the conventional one. The method is appreciably complicated in its mechanical aspect, but it has the great advantage of recording several reciprocal layers by a single exposure.

Introduction

In almost all moving film method only a particular set of reflections, such as (*hk*0) or (*hk*1) is allowed to fall on the film, and these are spread out over the film in such a way that each point on the photograph corresponds to a single value of *h*, and a single value of *k*. The Weissenberg method is the most common moving-film method which shifts the cylindrical film in a direction parallel to the rotation axis of the crystal. In this method, the crystal position as well as the diffraction angle is recorded on the synchronously moving film, and the unit cell dimensions or intensities of the diffracted rays are accurately determined by employing a back reflecting or an integrating type apparatus.

It is a distinct disadvantage of the conventional Weissenberg method, however, that only one reciprocal lattice plane can be photographed for each exposure, while other reflections are intercepted by the cylindrical screen. Because of this limitation, it is quite dif-

ficult to correlate the intensities of different layers, and also it is almost impossible to record under the same condition, a complete set of diffraction patterns of crystals of unstable state such as at high and low temperature, not to mention the inconvenience of the long time necessary to obtain the complete set of diffraction patterns.

Efforts have been made by various investigators in recent years to eliminate the above short comings while maintaining the essential functions of the Weissenberg method. H. P. Stadler[6] reported a double slit method which is very useful for comparison of the diffraction patterns of two reciprocal lattice layers on the same film. The interpretation of the film, however, is somewhat difficult and the back ground fogging is augmented because the reflections from both layers are superimposed on the same film. With this in view, W. R. Ruston[5] has adopted Stadler's method for the Unicam double-crystal Weissenberg goniometer. This method has the advantage of not augmenting the background fogging because both slits act as one full slit, but it is possible to record only two reciprocal lattice layers for each exposure with this apparatus.

The scope of the present paper is to discuss the techniques by which the zero to the n-th layer of the reciprocal lattice normal to the oscillation axis is recorded simultaneously, thereby greatly shortening the necessary exposure time.

The Spiral Weissenberg Apparatus

The writer designed, with the view of eliminating the difficulties of the conventional Weissenberg methods, a new technique in which several reciprocal lattice layers are recorded simultaneously on separate parts of a film. The difference of the direction of the film movement between the conventional Weissenberg method and the present one is shown in Fig. 1. There are several varieties for this method as shown in Fig. 2. In (A) of Fig. 2 is shown a technique using a photographic plate. This is mechanically the simplest method, but the interpretation of the diffraction patterns is more complicated

than that of a cylindrical film. Nevertheless, it may be practical with an X-ray radiation of comparatively short wave length such as molybdenum radiation. (B) shows a technique in which the film moves spirally around the surface of the cylindrical screen. It is disigned so that the film will not interfere with the collimater for the incident X-ray beam. This technique is very convenient for recording reflections with low value of ξ of high order layer lines. However it is difficult to record

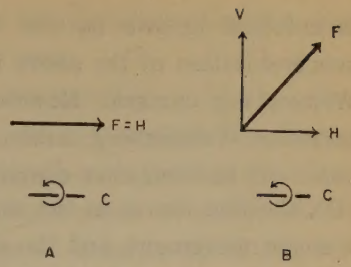

Fig. 1. The difference of the film movement between the conventional Weissenberg method (A) and the spiral new method (B).
C: crystal, H: horizontal direction, V: vertical direction, F: direction of the film movement.

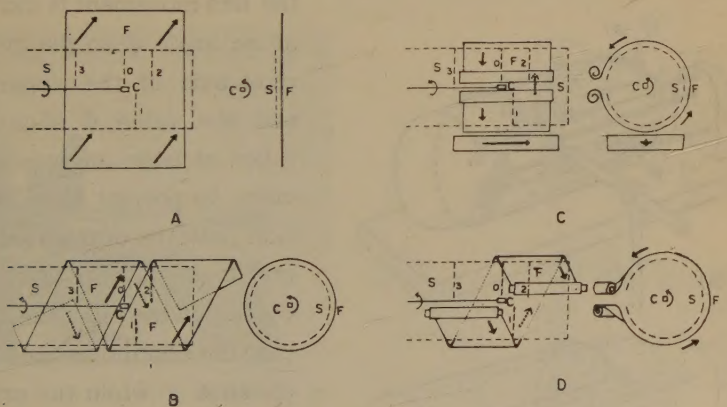

Fig. 2. Several techniques for the spiral Weissenberg method.
C: crystal, S: screen, F: film, 0~3: Slits for n-th layer line.

nesessary layer lines such as 0 layer, and it is mechanically unpractical to move the film in such a high pitch. The film movement of (C) is in the conbined direction of the linear motion similar to that of the conventional Weissenberg technique, and oscilatory motion around the circumference of the cylindrical screen. Both ends of the film

is enfolded in two parallel cylinders in this apparatus. A similar synchronization of the above movement is seen in the Integration Weissenberg camera. However the rotational movement of the Integration Weissenberg camera is not continuous and the above technique will be somewhat complicated mechanically. In the apparatus (D), the film moves in the same direction as in the case of (C) in a single movement, and the axes for enfolding the film are not parallel to the rotation axis of the crystal. In this technique, which the writer employed, the movement of the film is an oscillatory spiral motion over the surface of the cylindrical screen. Thus the writer proposes the name of spiral Weissenberg method for this technique.

The principle of this apparatus concerning the motion of the film holder and the arrangement of the screen slits is compared with that of the conventional Weissenberg method in Fig. 3. The direction of the film movement is inclined at an angle ϕ to the cylindrical axis of the apparatus and the value ϕ should be taken as large as possible in order to prevent the diffraction patterns of different layers from intersecting each other. In the most simplified case the film moves the linear distance z while the crystal rotates through an angle ω, and this relationship is the same as in the case of the conventional Weissenberg technique. In this case, both instrumental constants C_1 and C_2 are the same while the geometry of the diffraction

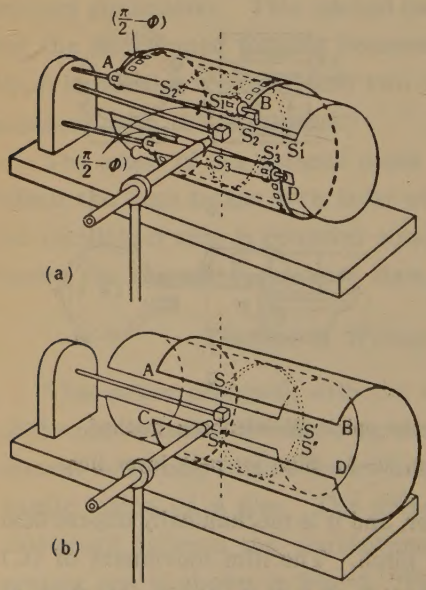

Fig. 3. Component parts of the spiral Weissenberg apparatus (a) and the conventional Weissenberg apparatus (b).

pattern is deformed by the direction of the movement of the film which is not parallel to the cylindrical axis.

It is necessary to wind both ends of the oscillating films in cylinders in the spiral Weissenberg method and it somewhat complicates the mechanism. In general, there is enough room between the X-ray tube and the Weissenberg apparatus to attach a pair of slightly slanting cylinders to the front of the camera in order to enfold the oscillating film. It may be more convenient to set these cylinders above, under or behind the apparatus. Furthermore, these cylinders, if necessary, can be separated in several packs, according to the reciprocal lattice layers.

The layer-line screens of this instrument consist of several full or half cylinders and they can be moved along a brass tube parallel to the rotation axis, to set the positions of layer line slits.

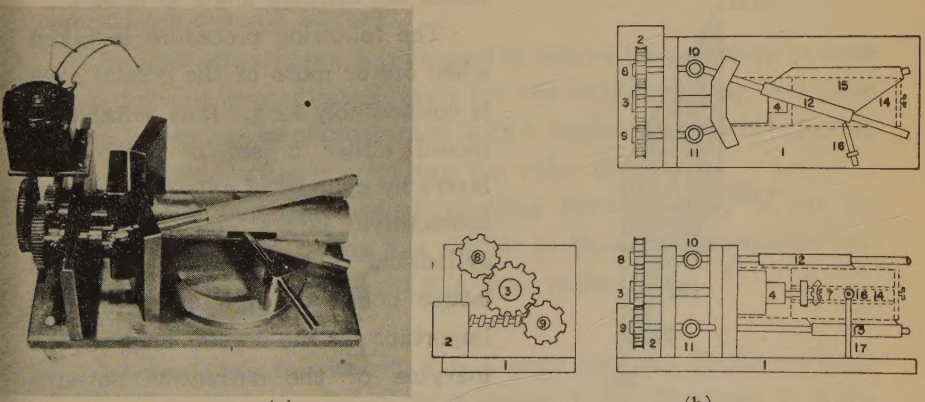

(a) (b)

Fig. 4. The model of spiral Weissenberg apparatus made in the writer's laboratory.

The model of the apparatus shown in Fig. 4 (a) was made in the writer's laboratory, and the plan, the elevation and a side view showing the gear mechanism are set out in Fig. 4 (b).

The cylinders for enfolding the film (12, 13) are synchronized with the oscillation of the crystal by gears (8, 3, 4, 9), and they are joined by universal joints (10, 11) so that the slanting angle Φ may

be taken arbitrarily.

With the present apparatus, it is not possible to record back reflections (*i. e.*, the reflections with high ξ), but the necessary layer lines can be photographed simultaneously. Therefore, when X-rays with relatively short wavelength such as molybdenum radiation are used, the layer lines can be recorded simultaneously by placing a film or plate normal to the incident X-ray beam and moving it in such a way that it cuts the cones of the layer lines obliquely.

Ordinarily, the incident X-ray beam makes an angle μ with the normal to the rotation axis, and the equi-inclination, the antiequi-inclination and the flat-cone positions are used for the n-th, 0, and $\frac{1}{2}$ n-th layers respectively. The general inclination position is used for other layers. The interpretation of these diffraction patterns should be referred to M.J.Buerger[4]. A template is shown in Fig. 5 in which the slanting angle Φ is 60°.

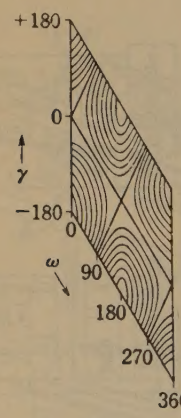

Fig. 5. A template for the spiral Weissenberg method.

The following procedure is taken when one or more of the crystal axes is considerably long. It is suitable to record either a set of alternative layers by cylindrical slits or a set of consecutive layers by using half cylindrical slits. When reciprocal lattice points of high order are not important for the crystal analysis, the margins of the diffraction patterns may be superimposed on the same part of the film.

Discussion

The spiral Weissenberg method has the great advantages of recording several layers of a reciprocal lattice simultaneously on separate parts of the film without increasing the background fogging, thus it enables the comparison of intensities of different layers on one film,

and it is possible to record a complete set of diffraction patterns of crystals in unstable states such as at high or low temperature etc., under the same condition.

On the other hand, this method has some shortcomings compared with the conventional Weissenberg method. Aside from the mechanical complexity, each area of the diffracted patterns is considerably small, thereby decreasing the accuracy of the measured values, and the interpretation of the patterns is a little more difficult.

The optimum values of the slanting angle and the coupling constant are calculated theoretically, but it may be necessary to alter the values according to the conditions of the experiment. For example, with the slanting angle of $\Phi=70°$ the corners of the diffraction patterns intercept each other if the intervals of the screen slits are within 15 mm.. On the contrary, when Φ is too large, the diffraction patterns are shortened in the direction of the oscillating axis and the experimental error would increase.

In most actual cases, it is unusual to require the recording of more than three reciprocal lattice layers for one oscillating axis, and these three layers can be photographed with a single exposure by selecting suitable layers without enlarging the value Φ.

There is also a method of recording several layers of the reciprocal lattice on a long film similar to those used in motion pictures. This will be discussed in a later paper.

In concluding this report, it is a great pleasure for the writer to express his sincere gratitude to Professor T. Ito, Professor T. Watanabe and Dr. R. Sadanaga of the Faculty of Science, University of Tokyo, who were generous in giving him valuable advice and suggestions. He is indebted to Dr. Y. Shimazaki for critically reading this manuscript. Thanks are also due to Professor N. Katayama, Professor S. Iwao and Dr. H. Minato, College of General Education, University of Tokyo, for their support, and to Kotoyo Takano, the Faculty of Science, University of Tokyo, for her assistance.

References

1) Böhm, J.: Z. Physik, **39**, 557 (1926).
2) Buerger, M. J.: X-ray Crystallography (New York, Wiley), 214; 296; 393 (1942).
3) Eichhorn, E. L. and K. Hoogsteen: Acta Cryst., **9**, 321 (1956).
4) Henry, N. F. M., H. Lipson and W. A. Wooster: The Interpretation of X-ray Diffraction Photographs, 87 (1953).
5) Ruston, W. R.: Acta Cryst., **4**, 473 (1951).
6) Stadler, H. P.: Acta Cryst., **3**, 262 (1950).
7) Straumanis, M., A. Ievins and K. Kalsons: Z. Physik. Chem. (B), **42**, 143 (1939).
8) Weissenberg, K.: Z. Physik., **23**, 229 (1924).
9) Wiebenga, E. H. and D. W. Smits: Acta Cryst., **3**, 265 (1950).

Manuscript received April 17, 1957

Mineralogical Journal, Vol. 2, No. 3, pp. 151-161, Dec., 1957

SERICITE FROM OZAWA-MURA, GUMMA PREFECTURE

Hideomi Kodama

Geological and Mineralogical Institute, Faculty of Science, Tokyo University of Education

Abstract

Mineralogical data of sericite found near the Yoji pass, Ozawa-mura, Kanra-gun, Gumma Prefecture, are reported in this paper. The material is white powder with silky luster and occurs as a hydrothermal alteration product of quartz-diorite. Specfic gravity is 2.87 The result of the chemical analysis is SiO_2 47.65, TiO_2 0.10, Al_2O_3 37.03, Fe_2O_3 0.01, FeO tr., MnO tr., MgO 0.04, CaO tr., K_2O 9.02, Na_2O 0.76 H_2O (+) 4.97, H_2O (−) 0.73, P_2O_5 0.02, total 100.33%, and this gives the structural formula of $(Na_{0.09}K_{0.76})Al_{2.00}(Al_{0.87}Si_{3.13})O_{10}(OH)_2$. The d.t.a. curve shows two endothermic peaks at 635°C. and 980°C.. X-ray studies of a pre-heated specimen revealed that the final destruction of the sericite lattice occurs at about 970° to 1,000°C., mullite appears at 1,000°C. and, that at 1,100°C. sericite is completely transformed into mullite. The (060) spacing is 1.501 Å., which indicates that the specimen is of the dioctahedral type.

Although the sericite leached by hot concentrated sulphuric acid displays X-ray powder lines different from those of original specimen, the results of acid treatment confirmed that the sericite is more durable than chlorite to acid attack.

Introduction

A few years ago, a sericite deposit was discovered by C. Kobayashi near the Yoji pass, Ozawa-mura, Kanra-gun, Gumma Prefecture (Fig. 1). The locality of this sericite deposit is about one kilometre northeast of the Yoji pass, just about ten kilometres east of Kaizé Station of the Koumi Railway Line.

The sericite has been investigated by thermal, chemical, X-ray and electron micrographic methods.

Fig. 1. Map showing the locality of the sericite from Ozawa-mura (×).

This paper gives its mineralogical data, with some considerations on the results of heat and acid treatments.

Mode of occurrence

The area around this sericite deposit is covered by the sedimentary rocks of the Uchiyama formation and a quartz-diorite mass. The former comprises argillaceous rocks, mainly shale, of Oligo-Miocene or Lower Miocene. The latter penetrating the former is remarkably brecciated, silicified, sericitized and pyritized, due to its endogenic alteration, partly giving rise to the formation of the sericite deposit. The intrusion of this igneous body was closely related to the formation of the Uchiyama fault, and it is presumed that the age of the intrusion is the Middle Miocene[9]. Andesite lava flows with distinguished platy joints cover these rocks.

Reference specimen

The specimen collected from the inner core of the irregular sericite mass assumes white powder with silky luster. The microscopic study confirmed that the crude clay containes very small a-

mounts of pyrite and fine dusty material. The specimen for experiments was prepared by removing pyrite by flutriation.

Differential thermal analysis curve

The differential thermal analysis curve recorded by the mean heating rate of 10~15°C. per minute is reproduced in Fig. 2. The thermogram of the sericite shows two endothermic peaks. The first appears between about 550°C. and 650°C. as a broad S-shape peak. The second is a small endothermic peak at about 980°C.. The former refers to the loss of OH, but the latter is not explainable at present.

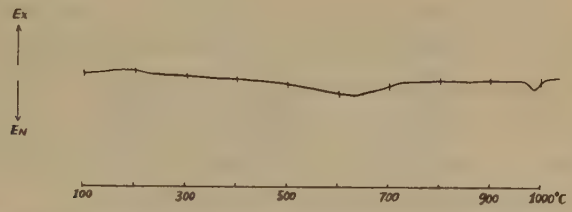

Fig. 2. Thermogram for the sericite from Ozawa-mura.

Electron micrograph

The electron micrograph of the present specimen shows that it consists of platy crystals with distinct hexagonal outlines[4]. Most of the flakes are from one to about five microns (Plate I, Fig. 3).

Chemical composition and structural formula

The chemical analysis of this sericite is given in Table 1. Sericite is known to have chemical composition similar to muscovite, except having less K_2O and more H_2O[5][6][7]. In Table 2, the relationship between the molecular proportions of typical muscovite, sericite and illite[6] are compared with those of the sericite now under consideration. It can readily be seen that the data of the present mineral agree well with those of the typical sericite.

From the analysis, the atomic ratio was calculated on the basis of 22 anions, $O_{10}(OH)_2$[8], as shown in the third column of the Table 1. The structural formula of the sericite can be written as follows:

$$(Na_{0.09}K_{0.76})\ Al_{2.00}\ (Al_{0.87}Si_{3.13})\ O_{10}\ (OH)_2.$$

Table 1. Chemical analysis and atomic composition of the sericite from Ozawa-mura.

	Wt. %	Mol. prop.	Atom. prop.	Atom. ratio
SiO_2	47.65%	0.793	0.793	Si 3.13 } 4.00
TiO_2	0.10			
Al_2O_3	37.03	0.363	0.726	Al 0.87 }
Fe_2O_3	0.01			Al 2.00 2.00
FeO	tr.			
MnO	tr.			
MgO	0.04			
CaO	tr.			
K_2O	9.02	0.096	0.192	K 0.76 } 0.85
Na_2O	0.76	0.011	0.022	Na 0.09 }
H_2O (+)	4.97			
H_2O (−)	0.73			
P_2O_5	0.02			
Total	100.33%			
S G	2.78			

Analyst: H. Kodama (1955)

Table 2. Table showing the relationship between the molecular proportions of typical muscovite, sericite and illite in comparison with those of the sericite from Ozawa-mura.

	Muscovite	Sericite	SERICITE**	Illite
SiO_2/R_2O_3	1.2	1.4	1.3	1.8
SiO_2/K_2O	7.0	9.5	9.3	12.7
R_2O_3/K_2O	3.2	4.0	4.1	4.6
(Fe, Mg) O*	26	39	n.d.	77
H_2O*	223	247	276	523

Note: * Molecular proportions are expressed with each value multiplied by 1,000.

** The specimen of sericite from Ozawa-mura.

X-ray diffraction data

X-ray powder diffraction data were obtained using Philips Geiger counter X-ray diffractometer. The experimental conditions are as follows: Ni-filtered copper radiation (Cu$K\alpha$, 1.5418Å), 35kV., 15mA., scanning speed 2°/m., scale factor 8, multiplier 1, time constant 4 seconds, receiving slit 0.006 inch.

The measured spacing and intensities are listed with the indices as 2M calculated by R. E. Grim in Table 3. The spacing of the (060) reflection (1.501Å.) suggests that the specimen is of the dioctahedral type. The b parameter can also be calculated from the chemical constituents of mica using the practical formula[3],

$b=\{8.90+0.12\ (Al^{3+})^{IV}+0.066(Mg^{2+})^{VI}+0.083(Fe)^{VI}+0.022(Ti^{4+})^{VI}\}kX$,

where $(Al^{3+})^{IV}$, $(Mg^{2+})^{VI}$, $(Fe)^{VI}$ and $(Ti^{4+})^{VI}$ indicate the number of each ion in the tetrahedral or octahedral coordination per half a unit cell. According to chemical data, number of $(Al^{3+})^{IV}$ is 0.87 and the third term and the followings are negligible. Therefore,

$$b=(8.90+0.12\times0.87)kX=9.02Å.$$

The result agrees fairly well with the value derived from (060) reflection as 9.01Å..

Table 3. X-ray powder data for the sericite from Ozawa-mura.

hkl	*d*	*I*	*hkl*	*d*	*I*
002	10.2 Å	80	$20\bar{2}$	2.57Å	30
004	5.07	50	008	2.51	10
110	4.51	30	$13\bar{3}$	2.462	10
	3.99	10	133	2.386	10
	3.90	10	043	2.137	10
023, 113	3.75	15	00,10	2.006	40
	3.51	15	$04\bar{6}$	1.737	10
006	3.36	100	312	1.653	20
114	3.21	15	13,10	1.528	10
	3.13	10	060	1.501	10
$11\bar{5}$, 025	3.01	30	00,14	1.431	5
115	2.88	15	$33\bar{7}$	1.356	15
$11\bar{6}$	2.81	10			

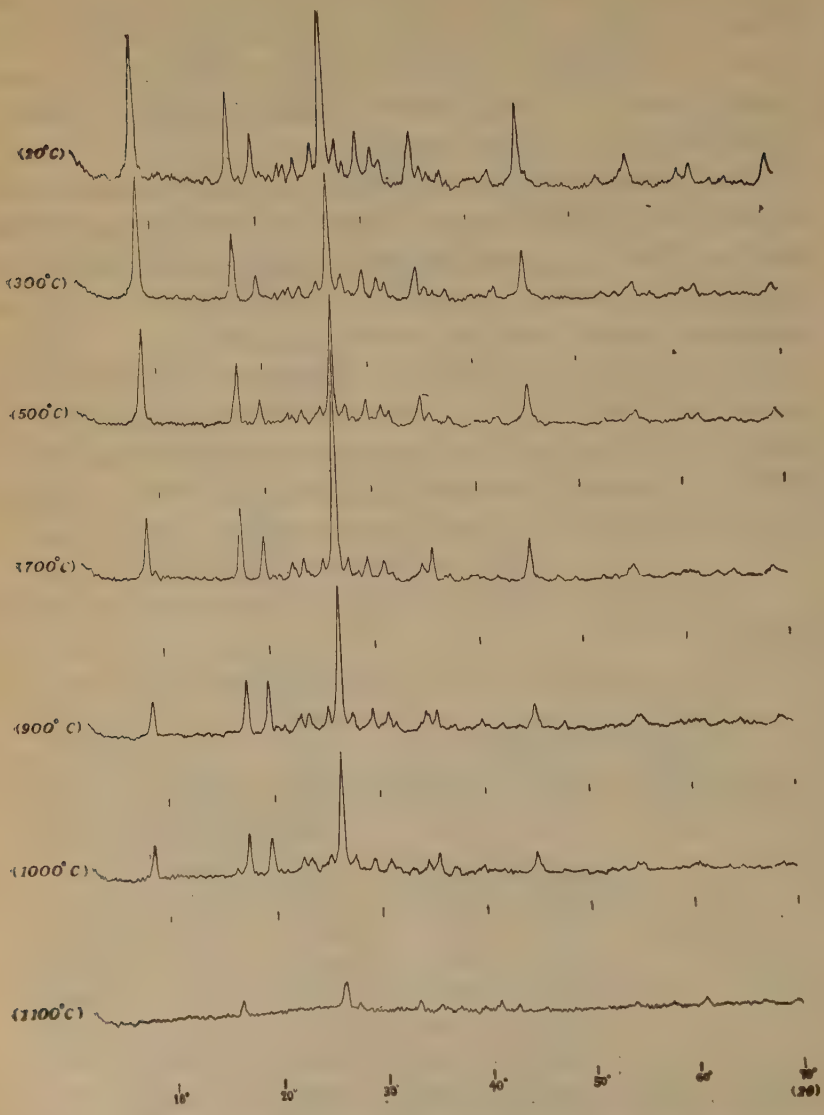

Fig. 4. X-ray powder diffraction diagrams for the sericite from Ozawa-mura and for the samples heated at various temperatures.

Effect of heat treatment

The present specimen was heated for an hour at 300°, 500°, 700°, 900°, 1,000° and 1,100°C., then was preserved in a glass vial until it was mounted on the X-ray apparatus. Most of the powder reflections of sericite are persistent in the pattern of the specimen heated up to 1,000°C. (Table 4. and Fig. 4). No obvious change is revealed in the diffraction pattern of specimen heated up to 500°C.. When heated at 700°C., the relative intensity of each of the (004), (006) and (008) lines becomes rather stronger than that of the corresponding lines of the specimen heated at 500°C.. It is presumed that the change depends on the transformation of dehydrated sericite into a new anhydrous modification.

Mullite appears at 1,000°C., which increases in amount until at 1,100°C., when sericite is completely transformed into mullite. Chemical process of this transformation may be represented as follows:

$$2(Na, K)Al_2(Al, Si_3)O_{10}(OH)_2 = \underset{\text{mullite}}{3Al_2O_3 \cdot 2SiO_2} + \underset{\text{amorphous alkali glass}}{(Na, K)_2O \cdot SiO_2} + \underset{\text{amorphous silica}}{3SiO_2} + 2H_2O.$$

Table 4. X-ray powder data for sericites unheated and heated at various temperatures.

A(20°C)		B(300°C)		C(500°C)		D(700°C)		E(900°C)		F(1000°C)		G(1100°C)	
d(Å)	*I*	*d*(Å)	*I*	*d*(Å)	*I*	*d*(Å)	*I*	*d*(Å)	*I*	*d*(Å)	*I*	*d*(Å)	*I*
10.2	80	10.2'	50	10.2	40	10.2	30	10.2	15	10.2	15		
												5.40	10
5.07	50	5.07	35	5.07	30	5.06	30	5.04	25	5.07	20		
4.51	30	4.48	10	4.51	10	4.51	20	4.51	25	4.51	20		
3.99	10	3.97	5	3.99	5	3.95	8						
3.90	10	3.90	5	3.92	5			3.92	10	3.92	5		
3.75	15	3.74	10	3.77	5	3.79	10	3.79	5	3.80	5		
3.51	15	3.50	10	3.52	10	3.52	5	3.52	10	3.53	5		
3.36	100	3.35	60	3.36	60	3.36	100	3.36	70	3.38	60	3.40	25
3.21	15	3.21	15	3.21	10	3.23	5	3.23	5	3.24	5	3.24	15
3.13	10												

A(20°C)		B(300°C)		C(500°C)		D(700°C)		E(900°C)		F(1000°C)		G(1100°C)	
d(Å)	*I*	*d*(Å)	*I*	*d*(Å)	*I*	*d*(Å)	*I*	*d*(Å)	*I*	*d*(Å)	*I*	*d*(Å)	*I*
3.01	30	3.00	15	3.00	10	3.03	10	3.03	10	3.04	5		
2.88	15	2.87	10	2.88	5	2.88	10	2.88	10	2.88	5		
2.81	10	2.80	10	2.81	5			2.81	5				
2.57	30	2.56	20	2.57	15	2.59	15	2.60	10	2.60	5	2.70	5
2.51	10	2.51	5	2.51	5	2.52		2.52		2.53	5	2.62	5
2.462	10	2.462	5										
2.386	10	2.386	5	2.398	5	2.410	5	2.410	5	2.417	5		
2.137	10	2.141	5	2.141	5	2.156	5	2.156	5	2.265	5	2.206	5
2.006	40	2.002	25	2.006	20	2.014	20	2.014	15	2.014	10	2.127	5
1.737	10	1.737	5	1.743	5	1.700	5	1.700	5	1.700	5		
1.653	20	1.647	10	1.650	5	1.670	5	1.670	5	1.670	5		
1.528	10	1.528	5	1.528	5	1.530	5			1.530	5	1.528	5
1.501	10	1.501	5	1.503	5								
1.431	5												
1.356	15	1.356	5	1.358	5	1.366	5	1.368	5				

Effect of treatment with acid

G. W. Brindley and R. E. Youell[1] tried to determine chemically, the tetrahedral and the octahedral aluminium ions in a chlorite. According to their experiment, chemical analysis of the material extracted from a chlorite by hydrochloric acid attack at constant temperature for various intervals revealed that the first stage of Al extraction is closely similar to extraction of other ions in the octahedral layer, but thereafter proceeds very slowly. If the limit of the first stage of the reaction is taken to represent the octahedral Al, then the ratio of tetrahedral to octahedral Al in the structure agrees closely with the ratio given by the structural formula. The agreement suggests that it may be possible to determine chemically, the amounts of tetrahedral and octahedral aluminium ions in a structure.

The writer tried to apply this method for the aluminium ions in sericite. A half gramme of the sericite was treated with considerable excess of 1:1 HCl on water-bath at controlled temperature between

90° and 100°C., for varying periods of time. Although the duration of treatment was prolonged up to thirty hours, Al extraction was nothing but a few per cent.. The result is different from that in the case of chlorite.

Next, sericite was treated with concentrated sulphuric acid at controlled temperature between 230° and 250°C. for suitable amount of time. After each treatment, the solid residue was filtered out,

Table. 5. X-ray powder data for five specimens treated with concentrated sulphuric acid at 230°~250°C.

1		2		3		4		5	
d(Å)	*I*	*d*(Å)	*I*	*d*(Å)	*I*	*d*(Å)	*I*	*d*(Å)	*I*
13.6	4	13.8	3	13.8	2.5	14.0	1.5	14.0	0.5
7.37	1.5	7.49	1.5	7.31	1			9.61	0.5
7.13	1.5	7.25	1.5						
5.90	1.5	5.94	1	5.94	1	5.94	2	5.90	0.5
5.01	1	5.01	1	5.01	1				
4.50	10	4.50	10	4.52	9	4.52	5	4.52	2
4.39	4	4.41	4	4.41	3.5	4.43	2.5	4.41	1.5
4.33	3	4.33	3	4.35	3	4.37	2	4.25	1
3.98	3	4.00	2.5	4.00	2	4.29	1.5	4.00	1
3.91	2	3.95	2	3.95	1.5	3.93	2		
3.69	1.5	3.70	1.5	3.70	1	3.69	1.5		
3.61	1.5	3.61	1.5	3.61	1				
3.52	4	3.52	2	3.53	1.5	3.53	5	3.53	2.5
3.46	1.5	3.46	1.5	3.46	1				
3.37	1.5	3.37	1.5	3.38	1	3.37	1	3.38	0.5
3.11	0.5	3.11	1	3.11	0.5	3.12	0.5		
3.02	1.5	3.03	1.5	3.03	1	3.03	1		
2.93	1	2.94	0.5	2.94	0.5	2.94	1	2.94	0.5
2.86	0.5	2.86	0.5	2.86	0.5	2.86	0.5		
2.67	1					2.68	0.5	2.67	0.5
2.62	1	2.64	0.5	2.64	0.5	2.62	0.5	2.62	0.5
2.57	0.5					2.58	0.5	2.57	0.5
2.50	1	2.50	1	2.50	0.5	2.51	0.5		
2.46	0.5	2.46	0.5						

1		2		3		4		5	
d(Å)	I	d(Å)	I	d(Å)	I	d(Å)	I	d(Å)	I
2.34	0.5	2.34	0.5						
2.04	0.5					2.05	0.5		
1.985	0.5	1.985	0.5	1.933	0.5				

1. 12% Al extracted specimen.
2. 22% Al extracted specimen.
3. 32% Al extracted specimen.
4. 61% Al extracted specimen.
5. 70% Al extracted specimen.

washed by water, dried at 70°C. and studied by X-ray method (Table 5). The filterate was prepared for chemical analysis.

The significant phenomenon is that the powder reflections different from those of the original specimen have been observed in the pattern of the specimen treated with hot concentrated sulphuric acid. Although the intensities of the new powder reflections decrease with increasing Al extraction, the new reflections are generally persistent in the pattern of the specimens with 70% or less Al extraction. When Al extraction amounts to about 90%, they are replaced by the pattern suggesting amorphous state.

Although the result obtained thus far is negative concerning the distinguishing of tetrahedral and octahedral aluminium ions in sericite, it arouses some crystallo-chemical interest. The writer is especially interested in the persistent powder lines displayed by the specimens treated with sulphuric acid, and is making an effort to clarify their nature, the details of which will be reported in the near future.

Acknowledgements

The writer wishes to express his sincere thanks to Prof. T. Sudo for his kind guidance and helpful advice during the course of this investigation. Thanks are also due to Prof. H. Shibata, Dr. K. Watanabe, Mr. S. Sato, Mr. R. Kuroda and many other persons at Tokyo University of Education, as well as to Prof. S. Iwao of University

Fig. 3. Electron micrograph of the sericite from Ozawa-mura.

of Tokyo for their valuable suggestions. Further the writer's cordial thanks are extended to Prof. C. Kawashima, who offered the electron micrograph, of Tokyo Institute of Technology and to Messrs. C. Kobayashi and K. Sakane who kindly assisted in field surveys and offered the specimen of sericite used in this work, and the Committee of the Norelco Geiger-Counter X-ray Diffractometer in University of Tokyo for giving him opportunities for using the apparatus.

REFERENCES

1) Brindley, G.W. and R.F. Youell: Acta Cryst., 4, 495 (1951).
2) Brindley, G.W.: Proceedings of the international symposium on the reactivity of solids, Gothenburg (1952).
3) Grim, R.E., W.F. Bradley and G. Brown: X-ray identification and crystal structure of clay minerals (1951).
4) Grim, R.E.: Clay Mineralogy (1953).
5) Otsu, H.: Bull. Geol. Surv Japan, 5, 583 (1954) (in Japanese).
6) Sudo, T.: Kagaku, 18, 172 (in Japanese).
7) Sudo, T.: Bull. Chem. Soc. Japan, 22, 25 (1948).
8) Sudo, T.: Nendo Kobutsu (Clay Mineralogy) (1953) (in Japanese).
9) Watanabe, K.: Memorial Volume dedicated to the late Prof. Kawada. (1954) (in Japanese).

Manuscript received April 19, 1957.

Mineralogical Journal, Vol. 2, No. 3, pp. 162-168, Dec., 1957

X-RAY SURFACE REFLEXION FIELDS ON PRECESSION PHOTOGRAPHS

Yoshio Takéuchi

Mineralogical Institute, University of Tokyo

Abstract

The areas of internal and surface X-ray reflexions on the precession photograph are theoretically derived for any crystal habit and are experimentally demonstrated as background patterns for two important cases. Considerations presented here seem to be useful for the estimation of absorption in precession photography.

Introduction

While an X-ray photograph of a crystal is being taken, the incident X-rays are scattered by the crystal surfaces and soft, incoherent radiations are produced. Some parts of these incoherent radiations reach the film, while a part is effectively screened by the crystal, and the total effect results in a background pattern of surface reflexions.

With the precession method, it is always possible to find an appropriate tilt angle so as to minimize the exposure time to record the required part of the reciprocal lattice, and consequently, the chances of observing background patterns are comparatively rare. However, even in this method, longer exposures make it possible to record the patterns, and therefore, it seems worthwhile to develop the systematic interpretation of these patterns, especially in connection with absorption correction, as treated in this article. A detailed account for the Weissenberg photograph has been given by M. J. Buerger[1].

Theoretical consideration of the fundamental case

A case which is fundamental to the development of more com-

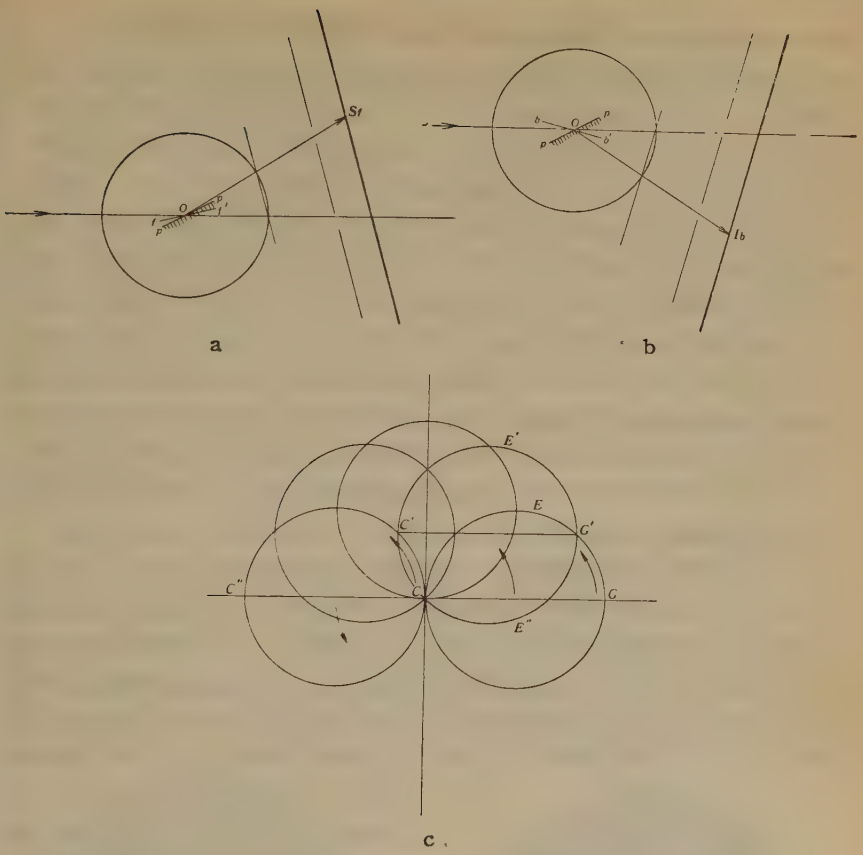

Fig. 1. a and b. Diagramatic representation of surface and internal reflexions. c. The process of the development of surface reflexion field on the precession film.

plicated cases is that of a crystal with one plane surface parallel with the cone axis of precession. For the sake of simplicity, the extension of the surface is assumed to be infinite. A diagramatic representation of this case is given in Fig. 1a. The incident X-ray beam strikes the plane surface of the crystal, pp, at its intersection with the precession axis, O. Under these circumstances, the surface and internal reflexions are defined as follows.

The surface reflexions are those reflected by planes, like ff', above

the crystal surface towards the semi-circle C′E′G′ (Fig. 1c), to S_f for example, where C′G′ being the line of intersection between the extention of the surface pp and the plane of the film. For such reflexions, neither the incident nor the reflected beam penetrates any appreciable body of the crystal before it reaches the film. On the other hand, planes, like bb′, reflect the beam towards the other half of the circle, to I_b for example (Fig. 1b). Such reflexions are termed internal reflexions and are recorded after either the incident or the reflected beam has travelled all the way through the crystal body. If the crystal shows high absorption, internal reflexions will be severely reduced in intensity. It is evident from Fig. 1c that the direction of surface reflexions lies on the semi-circle C′E′G′, the intersection of the diffraction cone with the precession film, and that of internal reflexions the other half of the circle, C′E″G′.

Now, when the precession movement brings the crystal to a position where the plane under consideration is parallel with the incident beam, surface reflexion begins from that instant and is recorded along the semi-circle CEG on the film (Fig. 1c). As the precession continues, the semi-circle traverses the film with the speed of the precession and the both ends of line CG move along the semi-circles CC′C″ and GEC respectively. After CEG has been brought to the position of CC′C″, surface reflexion is no longer possible because the surface falls into the shadow of the crystal body in respect of the incident X-ray beam. Thus, the semi-circle C EG sweeps over part of the film surface and develops a fan-shaped surface reflexion area, CC″E′G, as shown in Fig. 2.

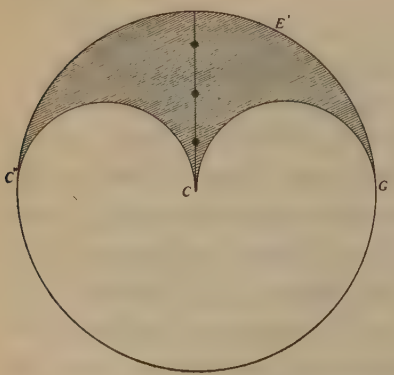

Fig. 2. Shaded area represents the surface reflexion field from the single crystal surface.

Application of the theory to more complicated cases

1. *Crystals with more than two surfaces parallel with the cone axis of precession.*

From the above discussion, the shape of the surface reflexion field for crystal with more than two surfaces, each parallel with the cone axis of precession, can easily be derived. Suppose that a crystal has, in its zone parallel with the cone axis, n natural faces of angular coordinates ω_1, ω_2, ω_3.....ω_n. As precession movement brings each of these successively parallel with the incident beam, its semi-circular surface reflexion starts to form fan-shaped areas identical with those illustrated in Fig. 2. As the result of a complete cycle of the precession, therefore, a composite surface reflexion field, consisting of n individual areas, develops on the film.

Simple composite cases with ω=180° (tabular habit with negligible edge faces), ω=120° (trigonal prism) and ω=90° (tetragonal prism or cube) are shown in Figs. 3, 4 and 5 respectively. An example of more generalized case such as a crystal having two pairs of pinacoids in its zone parallel with the cone axis is illustrated in Fig. 6. Any other composite cases and the case of a higher level photograph

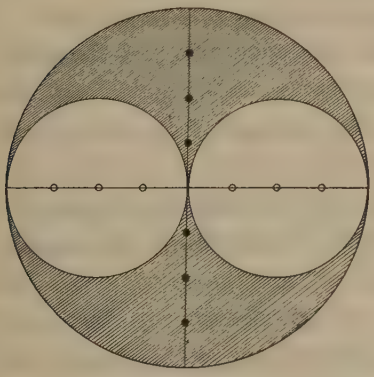

Fig. 3. Surface reflexion fields from a thin crystal plate in the zone of cone axis.

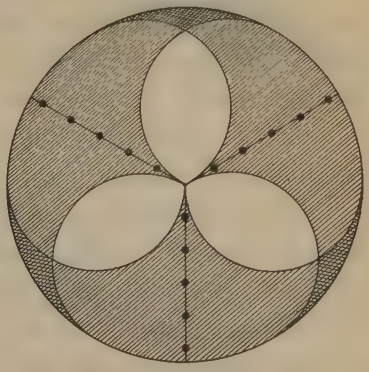

Fig. 4. Surface reflexion fields from trigonal prism in the zone of cone axis.

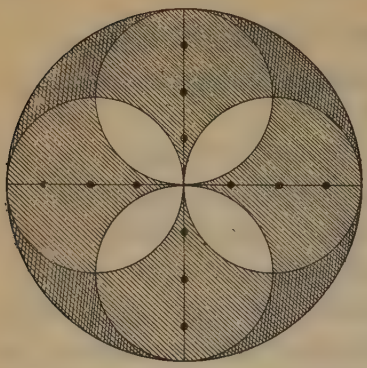

Fig. 5. Surface reflexion fields from tetragonal prism in the zone of cone axis.

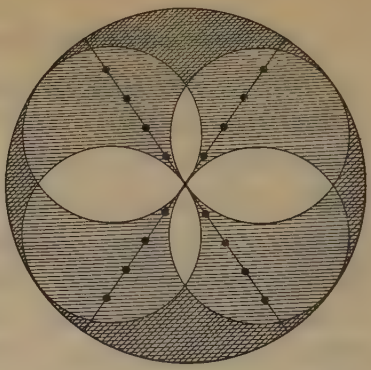

Fig. 6. An example of general cases. Surface reflexion fields from a crystal bounded by two pairs of pinacoids, at ω intervals of 68° and 112°.

may be derived in the similar way.

2. *Crystals with surfaces not parallel with the cone axis.*

The surface reflexion areas of the surfaces which are not parallel with the cone axis are smaller than those of the foregoing cases.

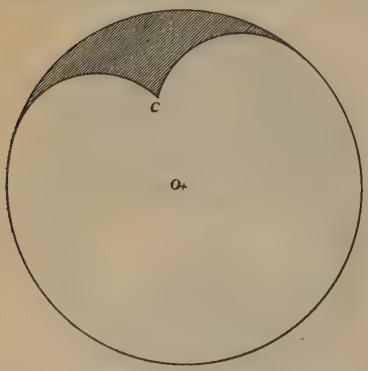

Fig. 7. Surface reflexion field from a crystal surface not parallel with the cone axis.

If a crystal bears a surface whose normal makes an angle, ρ, with the cone axis and the angle lies in between 90° and $90° - \bar{\mu}$, the surface reflexion from the surface can be recorded on the film. An example for this case is given in Fig. 7. The distance between the point, C, and the center of the film, O, varies according to the angle ρ. By measuring the value of CO, the angle ρ may be evaluated from the equation,

$$\rho = \cos^{-1}\frac{CO}{2F}$$

where F is the crystal-to-film-center distance.

Background pattern and the absorption corrections

The areas derived as surface reflexion areas can experimentally be made to appear on precession films as background patterns. Two of these are illustrated in Plate I, Fig. 8 and Plate II, Fig. 9.

To obtain background patterns for the purpose of comparing them with the theoretically derived surface reflexion areas, it is better to employ radiation whose wave length is just below the absorption edge of one of the elements present in the crystal, because, under such conditions, the scattering can be made especially intense. The amount of background blackening produced by any one crystal face is proportional to the area of the face included in the X-ray beam. However, with the precession method, only a small region of the crystal is explored by the beam. Therefore, it requires long exposure to obtain the blackening in the precession film. Indeed, the effect of the surface scattering on the precession photogrphs is surprisingly smaller than that of the Weissenberg photographs for a given exposure time.

The knowledge of the surface reflexion area is useful to the theory of absorption corrections as already discussed by Buerger for the case of Weissenberg photographs. It is clear from the above discussion that in the simple case, namely the thin crystal plate, all diffraction in the entire unshaded areas of Fig. 3, are subjected to important absorption. In the unshaded area, extreme absorption occurs along the margine of the circle and decreases towards inside of the circle, as the path of transmission decreases. Thus it may be possible to prepare a chart for this area giving the correction for absorption in precession photographs. A similar chart for the shaded areas of surface reflexions may also be prepared.

For the more general case as shown in Fig. 6, the correction

factor is more complex. However, it appears that these composite diagrams will be of considerable help for determining the appropriate absorption correction factor to be applied for any reflexion, because the diagrams reveal the surface and internal reflexion areas at a glance.

Acknowledgement

I am grateful to Prof. T. Ito and Dr. R. Sadanaga for their guidance and to Mr. Y. Iitaka for some helpful discussions.

References

1) Buerger, M. J.: Z. Krist., **99**, 189 (1938).

Manuscript received September 15, 1957.

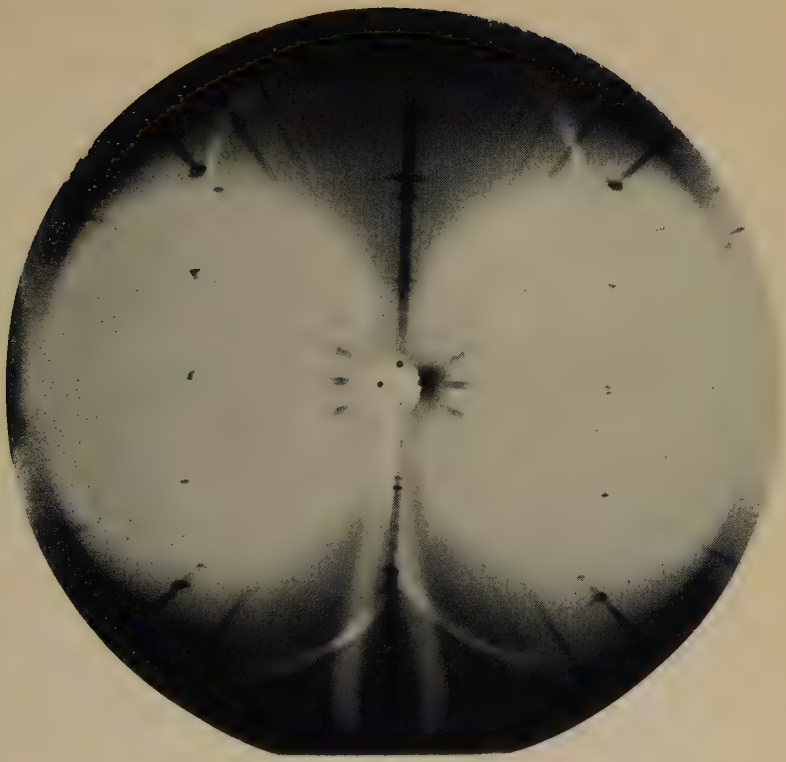

Fig. 8. Cobaltite, CoAsS, cube edge precession photograph with $\bar{\mu}=30°$. CuK radiation, 35 kV., 10 mA., 20 hours. Background pattern due to thin cleavage plate. Compare with theoretical background, Fig. 3.

Fig. 9. Pyrites, FeS_2, cube edge precession photograph with $\bar{\mu}=30°$. CuK radiation, 35 kV., 15 mA, 16 hours. Background pattern due to four cube faces in the zone of cone axis. The crystal used is a cube with edge dimension of about 0.4 mm.. Compare with theoretical background, Fig. 5.

MINERALOGICAL JOURNAL, VOL. 2, NO. 3, PP. 169-179, DEC., 1958

LONG SPACING CLAY MINERAL FROM THE UKU MINE, YAMAGUCHI PREFECTURE, JAPAN*

TAKESHI MITSUDA

Department of Geology and Mineralogy, Faculty of Science, Hokkaido University

ABSTRACT

A white powdery clay mineral with 28.8Å. spacing was found in the kaolinite vein of the Uku mine, Yamaguchi Prefecture. The interplaner spacings of stronger X-ray powder diffraction lines of the mineral are as follows: 28.8±0.1, 14.5±0.1, 4.82±0.02 and 1.4893±0.0005Å.. The 14.5Å. line shifts to 15.4±0.2Å. and the 28.8Å. line to 31.0±0.5Å. after treatment with ethylene glycol. The 28.8Å. line is persistent in the temperature range from 20° to 300°C., but completely disappears above 400°C.. The 14.5Å. line is replaced by the 12.4Å. line at 400°C., which is persistent up to 600°C. but disappears above 700°C.. At 1200°C. the specimen is transformed to mullite.

It is considered that, as T. Sudo et al. have already pointed out, the unusually long spacing of 28.8Å. is the result of a regularly alternating stacking of two kinds of layer lattices; one is the ordinary montmorillonite lattice with the basal spacing of about 14.8Å. and the other is a hypothetical aluminium chlorite lattice with the basal spacing of about 14.0Å..

Introduction

The clay mineral with long spacing of about 30Å. has been found in the clays from the Kurata mine, Yamaguchi Prefecture by T. Sudo, H. Takahashi and H. Matsui[4], from the Hanaoka mine, Akita Prefecture by T. Sudo and H. Hayashi[5], and from the Kamikita mine, Aomori Prefecture by T. Sudo, H. Hayashi, H. Kodama and K. Oinuma**. Recently the writer found a similar clay mineral from the

* Read at the Annual Meeting of the Mineralogical Society of Japan held in Tokyo on June 1, 1957.

** Refer to their paper read at the Annual Meeting of the Mineralogical Society of Japan held in Tokyo on June 1, 1957.

Uku mine, Abu-machi, Yamaguchi Prefecture*. In the mode of occurrence, the Uku clay especially resembles the Kurata fire clay, both occurring in veins mainly composed of kaolinite.

A detailed study of the 30Å. clay mineral was first attempted by T. Sudo et al.[4)5)], who interpreted that the 30Å. spacing is due to a regularly alternating stacking of two kinds of layer lattices; one is the ordinary montmorillonite layer lattice with the 15.4Å. spacing, while the other is a hypothetical one with the 14.0Å. spacing composed of a gibbsite and a pyrophyllite layers.

Mode of occurrence

As shown in Fig. 1 the ore bodies of the Uku mine are of lenti-

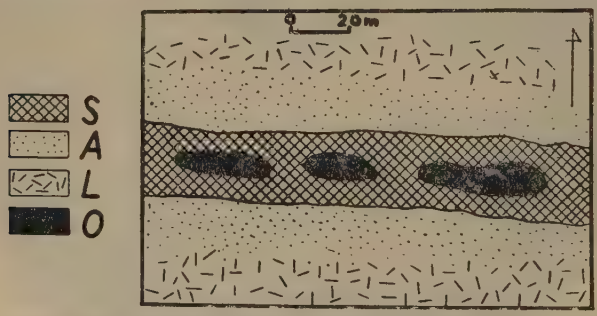

Fig. 1. Distribution map of country rocks and ore bodies of the Uku mine.
S: silicious rock.
A: altered zone largely composed of sericite.
L: liparite.
O: ore bodies largely composed of andalusite.

cular shape, embedded at intervals in silicious rocks which extend east and west, and they are composed of andalusite, corundum and sericite, with small amounts of pyrophyllite, quartz, rutile and pyrite. Although almost all of these minerals are unaltered, in places, aluminous silicate minerals have altered to clay materials due to later hydrothermal actions. On the basis of the differential thermal analysis and X-ray powder data, the clay materials were identified to

* 山口県 阿武町 字久鉱山.

be composed of kaolinite, diaspore and pyrophyllite.

The mode of occurrence of kaolinite veins including the long spacing clay mineral in question can be classified into two groups: one occurs as irregular network veinlets in flinty rocks and the other as a vein filled by powdery clay as illustrated in Fig. 2. When the

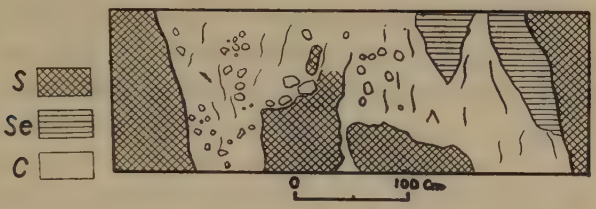

Fig. 2. Cross section of a clay vein in silicious rock.
S: silicious rock.
Se: sericite.
C: white powdery clay largely composed of kaolinite.
Sample (A) including the 29Å. clay mineral was collected in this vein.

clay mineral of the latter group was treated with saturated aqueous solution of benzidine, some of it became slightly green. It is worth noticing that montmorillonite is generally tinged with green by benzidine.

The long spacing at about 29Å. was observed in the X-ray diffraction pattern of sample (A) separated from the clay which was tinged with green by benzidine.

X-ray diffraction data

The X-ray powder patterns of the clay specimens of the Uku mine were obtained by Philips Geiger Counter X-ray Spectrometer with filtered Cu $K\alpha$ radiation. The experimental conditions were as follows: 35kV., 13mA., time constant 4 seconds, scanning speed 2° or 1/4° per minute, angular aperture 1°, receiving slit 0.006 inch.

Spacings of the principal powder lines with 2θ angle lower than 8° were accurately determined either by recording the reflection lines under scanning speed 1/8° per minute with angular aperture

1/4°, or by calibrating their angles by referring to the powder lines of quartz or silicon, and further by counting their intensities at the fixed time of 64 seconds with scale factor 8.

X-ray powder diffraction at room temperature

The X-ray powder diffraction patterns of sample (A) are depicted in Fig. 3 and correlated in Table 1 to those of kaolinite, sericite, pyrophyllite and quartz except the 28.8 and 14.5Å. lines. The reliability factors of their spacings are shown in Table 2.

The results are summerized as follows:

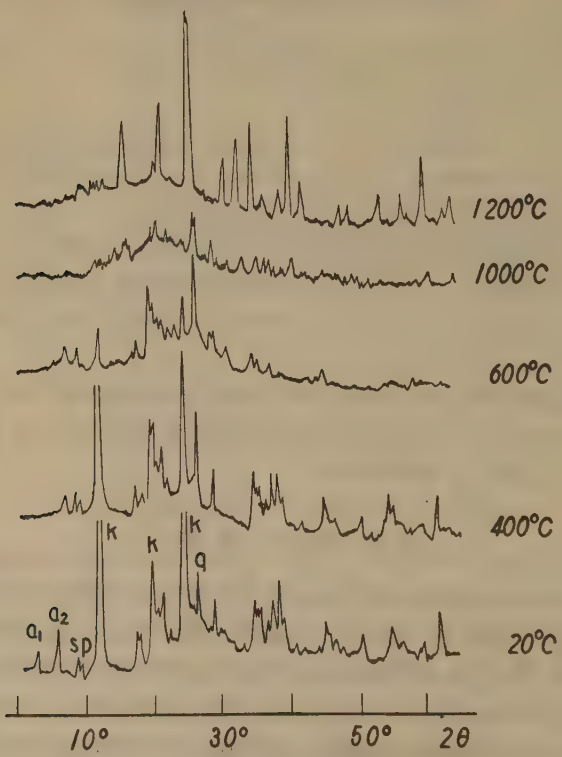

Fig. 3. X-ray diffraction patterns of sample (A).
a_1, a_2: 00*l* reflections from a basal spacing of 28.8Å.
K: kaolinite, q: quartz, S: sericite, P: pyrophyllite.

(1) It is clear that sample (A) is mainly composed of kaolinite with basal reflection of 7.17Å. (001), 3.578Å. (002) and 2.390Å. (003), which is of slightly disordered type as revealed by unification of the close doublet, $(1\bar{1}\bar{1})$ and $(11\bar{1})$.

(2) The 14.5, 4.81, 4.61 and 2.30Å. lines approximate to the reflections of montmorillonite, while the 14.5, 7.17 and 4.81Å. lines approximate to the subsequent reflections of the 28.8Å. line.

(3) The 4.26 and 3.34Å. lines imply the presence of small amounts of quartz, 10.0, 5.00 and 3.34Å. lines, that of sericite, and the 9.24Å. line that of pyrophyllite.

(4) The spacing of (06) or (060) is 1.489Å., which is similar to that of kaolinite and/or montmorillonite. It indicates that the principal clay minerals in sample (A) are of the dioctahedral type and that the number of aluminium ions in the tetrahedral coordination in the silica layer is quite small.

Effect of heat treatment

To ascertain the nature of the X-ray reflection of 28.8Å. spacing, the effect of heat treatment on X-ray powder pattern was investigated. Sample (A) was heated for one hour at every hundred degree interval between 100° and 1200°C. and each of the heated sample was examined by X-ray powder method after cooling to room temperature in the air.

The results obtained are shown in Fig. 3 and Table 1, and summerized as follows:

(1) It is the most important feature that the 28.8Å. spacing is unaffected up to 300°C., and on further heating at 400°C. the 28.8Å. line disappears completely and the 14.7Å. line is replaced by the 12.4Å. line, which is preserved up to 600°C. but absolutely disappears above 700°C..

(2) The pattern of kaolinite almost disappears at 600°C. and completely at higher temperatures.

(3) In the temperature range of 20°~900°C., the structures of

Table 1. X-ray diffraction data for sample (A)

d(calc.) for	S	P	K	Q	20°C		300°C	
$d(00l)=28.8_5$Å	*hkl*	*hkl*	*hkl*	*hkl*	d(Å)	*I*	d(Å)	*I*
28.85Å					28.8_5**	6	28.8*	5
14.43					14.5_2**	17s	14.4*	9s
	002				10.0_4*	8s	10.1	6s
9.62		002			9.24_3*	5s	9.2	4
7.21			001		7.17_2*	200s	7.16	170s
5.77	004				5.00_6*	15s	5.01	10s
4.81					4.81_9*	13	4.83	9
					4.61_5*	6	4.60	5
	110		020		4.45_7*	40s	4.45	40
			$1\bar{1}0$		4.37_9*	22	4.37	30
				100	4.26_9*	27	4.25	28
4.12			$11\bar{1}$ / $1\bar{1}1$		4.14_2*	15	4.14	14
3.606			002		3.57_8*	180s	3.58	150s
		113		101	3.340*	15s	3.34	10s
2.885	$11\bar{5}$ / 025				2.976*	15s	2.97_6	11s
	$20\bar{2}$		$20\bar{1}$ / 130		2.575* / 2.540*	20 / 4	2.57_5	23
			$13\bar{1}$		2.505*	16	2.508	20
			200		2.440*	11	2.400	10b
			003		2.390*	20	2.396	20
			$20\bar{2}$ / 131		2.342*	28	2.351	25
					2.301*	11	2.301	14
			$20\bar{3}$ / 132		2.00*	10b	2.000	10b
			$13\bar{3}$		1.943*	4	1.948	4
			004		1.792*	10	1.795	7
			$20\bar{4}$		1.662*	14	1.666	13b
			133 / 310		1.622*	5	1.659 / 1.622	11b / 7b
			203		1.545*	5	1.544	4b
			060 / $13\bar{1}$		1.489*	17s	1.489	20s

**: Spacing determined on the basis of the data of fixed time operation.

*: Spacing read on the chart recorded under the scanning speed 1/4° per minute.

Other spacings were read on the chart recorded under the scanning speed 2° per minute.

Relative intensities were estimated by amplitudes of peaks.

500°C		600°C		900°C		1000°C		1200°C	
d(Å)	*I*	*d*(Å)	*I*	*d*(Å)	*I*	*d*(Å)	*I*	*d*(Å)	*I*
12.4*	8b	12.4*	10b					5.41_3	26s
10.1	8s	10.1	10s	10.2	5			4.27_5	10
9.24	4s							4.09_9	31s
7.16	170s	7.16	15s					3.42_9	67
5.01	90s	5.01	8s	5.05	10s			3.40_8	63
								2.89_8	15s
?	?							2.70_0	27s
4.47	32s	4.50	30s	4.50	20s			2.55_0	33s
4.37	20	4.37	20					2.43_8	8
4.24	20	4.24	20	4.24	18	4.25	17	2.29_2	11
4.14	14							2.208	40
3.58	160s	3.58	20					2.127	15
3.34	25s	3.34	25s	3.34	45s	3.14	13vb	1.891	6
2.97	12	3.1	8b	3.11	11s	3.11	7	1.844	7
2.57	18	2.59	7			2.70	6b	1.712	11
2.508	15					2.53	5b	1.602	11
2.433	10					2.46	5b	1.527	26s
2.390	20							1.460	5
2.341	20							1.445	13
2.301	8								
2.000	12	2.000	6						
1.948	4								
1.795	7								
1.666	12b								
?	?								
?	?								
1.487	13					1.445	6		

s: sharp, b: broad, vb: very broad.
Q: quartz, K: kaolinite with indices after G. W. Brindley[1], P: pyrophyllite with indices after J. W. Gruner[3], S: sericite with indices after R. E. Grim[2].

sericite, pyrophyllite and quartz are not destroyed.

(4) The powder pattern of the sample heated at 1200°C. is similar to those of mullite.

Effect of treatment with ethylene glycol and/or water

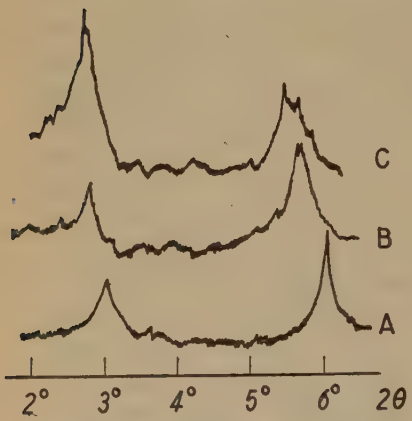

Fig. 4. Basal X-ray diffraction patterns for sample (A).
A: natural, B: complexed with ethylene glycol, C: complexed with water.

The original sample (A) was pulverized, then covered completely with a few drops of ethylene glycol and/or water on slide-glass. The treated samples were studied by X-ray powder method, and the results obtained are shown in Fig. 4 and Table 2; they may be summerized as follows:

(1) The 14.5Å. spacing expands to 15.4Å. with ethylene glycol; this amount of expansion is less than that of the montmorillonite with two sheets of water molecules. While,

Table. 2. Basal X-ray diffraction data for long spacing clays.

	Kurata[4]		Hanaoka[5]		Uku	
	d	*I*	*d*	*I*	*d*	*I*
(001)	29.8±0.5 Å	10s	29.6±0.2Å	10s	28.8 ±0.1Å	6
(002)	14.7±0.2	15s	14.7±0.1	18s	14.5±0.1	17s
(003)	10.3?	4b	9.8±0.1	3		
(004)	7.18±0.04	20s	7.32±0.02	5	7.17±0.02	200s
(005)	?		5.99?	3	?	
(006)	4.95±0.05	10s	4.91±0.02	10s	4.82±0.02	13
(009)	3.32±0.02	6b	3.30±0.02	5	?	
(00, 10)	3.03±0.06	4b	2.97±0.06	2	2.97±0.01?*	15s
(060, 331)	1.4919±0.0002	15s	1.5057±0.0008	8s	1.4893±0.0005	17s

* The spacing 2.97Å is superposed by that of sericite.

Complexed with ethylene glycol

	Kurata	Hanaoka	Uku
(001)′	32.3±0.5Å	31.6±0.2Å	31.0±0.5Å
(002)′	15.6±0.3	15.6±0.1	15.4±0.2

the 28.8Å. spacing expands to 31.0Å. at the rate twice as great as in the case of the 14.5Å. spacing.

(2) Upon treatment with water, the 14.5Å. spacing expands to about 16Å. and that of 28.8Å. to 31~32Å..

These facts suggest that 28.8Å. and 14.5Å. lines may be related to the presence of the montmorillonite lattice.

Differential thermal analysis curve

Heating rate for differential thermal analysis was 10°C. per minute. The differential thermal analysis curve of sample (A), as shown in Fig. 5, displays the following peaks:

(1) A clear endothermic peak in the temperature range of 100°~200°C. and a weak one in 200°~300°C..

(2) A sharp endothermic peak at about 600°C. and a broad weak one in the temperature range of 700°~800°C..

(3) Finally, a sharp exothermic peak in the range of 900°~1000°C.. Those peaks reveal that sample (A) includes both kaolinite and montmorillonite.

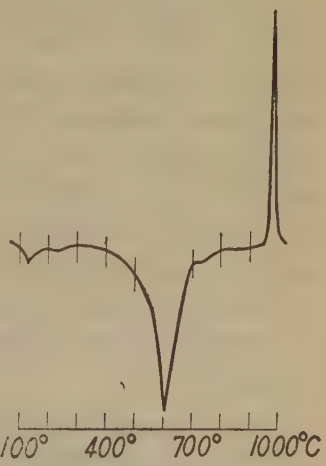

Fig. 5. Differential thermal analysis curve for sample (A).

Chemical analysis

The chemical analysis of sample (A) gave the following results: SiO_2 45.83, Al_2O_3 40.37, Fe_2O_3 0.61, TiO_2 0.11, CaO 0.15, MgO 0.07, K_2O

and Na_2O trace, $H_2O(+)$ 12.49, $H_2O(-)$ 0.85, total 100.48% (analyst, Goro Shibuya).

Taking into consideration the fact that the intensity of the 7.17Å. line of sample (A) is the strongest as well as the chemical composition of the sample, it may be concluded that the most dominant component of the Uku clay is kaolinite.

Discussion

The observed spacings of the long spacing clay minerals from Kurata[4], Hanaoka[5] and Uku are compared in Table 2. They are generally in good agreement with each other, but differ slightly with regard to their relative intensities as well as to the spacing of (001).

The spacing of (001) of the clay mineral from Uku is a little smaller than that from Kurata or Hanaoka. It may be considered that the montmorillonite layer composing the clay minerals from Kurata and Hanaoka have the basal spacing of 15.4Å. with two sheets of water molecules, whereas that from Uku, 14.8Å.. Actually, a certain specimen from the same locality as sample (A) produced a diffraction line at 14.8Å. while lacking the long spacing of about 29Å.. The 14.8Å. spacing of this specimen was identified as the basal spacing of montmorillonite by means of X-ray and thermal studies.

Accepting T. Sudo's idea on the 30Å. clay mineral, the long spacing observed for the sample from the Uku mine may be interpreted as follows:

The long spacing of 28.8Å. is caused by a regularly alternating stacking of two kinds of layer lattices: one is the usual montmorillonite lattice with about two sheets of water molecules and a cell height of 14.8Å. which is expected to decrease to 10.8Å. by dehydration and to expand to about 17.0Å. by the treatment with ethylene glycol; the other is an aluminium chlorite lattice with a cell height of about 14.0Å. which is expected to be unaffected by the treatment with ethylene glycol and/or water and may be persistent at least up to 600°C..

Acknowledgements

The writer is greatly indebted to Professor Zyunpéi Harada, Hokkaido University, for reading this manuscript and offering significant suggestions. Thanks are due to Professor Toshio Sudo, Tokyo University of Education, for helpful suggestions, and to Mr. Goro Shibuya, Yamaguchi University for chemical analysis. The writer also acknowledge to Mr. Hiroshi Noguchi, the President of the Nihon Firebrick Company for affording facilities for field survey.

REFERENCES

1) Brindley, G. W.: X-ray identification and crystal structures of clay minerals, (1951).
2) Grim, R. E., R. H. Bray and W. F. Bradley.: Amer. Miner., **22**, 813 (1937).
3) Gruner, J. W.: Zeit. Krist., **88**, 412 (1934).
4) Sudo, T., H. Takahashi and H. Matsui: Nature, **173**, 261 (1954).; Jap. Journ. Geol. Geograph., V, **24**, 71 (1954).
5) Sudo, T. and H. Hayashi: Science Reports of the Tokyo Kyoiku Daigaku, C, No. 25 (1955).

Manuscript received September 28, 1957.

MINERALOGICAL JOURNAL, VOL. 2, NO. 3, PP. 180-186, DEC., 1957

A NEW OCCURRENCE OF PYROSMALITE IN THE KYURAZAWA MINE, TOCHIGI PREFECTURE, JAPAN

TAKEO WAKANABE and AKIRA KATO

Geological Institute, Faculty of Science, University of Tokyo

ABSTRACT

Pyrosmalite, $(Fe, Mn)_8 Si_6O_{15} (OH, Cl)_{10}$, occurs abundantly as an important ore-forming mineral at the Kyurazawa mine, Tochigi Prefecture. It is hexagonal, with $a_0 = 13.40$Å. and $c_0 = 7.135$Å. The tabular or prismatic crystals are often found in vugs in the coarse granular aggregate of pyrosmalite and knebelite.

Basal cleavage is perfect, $\omega = 1.671$, $\varepsilon = 1.639$, uniaxial negative; Sp. G. = 3.14. More than 1500 tons of the manganese-iron ore containing 23-24% Fe and 24-23% Mn, and consisting of knebelite, pyrosmalite and the other manganese silicate minerals have been shipped from this mine for metallurgical uses since August, 1956.

Introduction

The occurrences of pyrosmalite have been recorded from Sterling Hill, New Jersey[1] and Broken Hill, New South Wales[2][3] and the other old known localities in Sweden.

The first occurrence of pyrosmalite in Japan was recognized by the writers in the specimens of iron-manganese ore from the Kyurazawa mine, which were collected by Mr. B. Gokan in August, 1957. The mineral was indentified by X-ray powder and optical methods.

In November, 1957, the writers visited the mine and could collect many specimens of pyrosmalite. It is very interesting to notice that such rare mineral as pyrosmalite is so common and abundant and that it has been regarded as one of the important ore minerals in the mine.

Occurrence and paragenesis

The Kyurazawa mine* is located in the manganese area of the Ashio Mountain District[4] about 2.5 km. south-east of Ashio Town, the famous copper mining center in Tochigi Prefecture, Japan. Its principal ore bodies are distributed in a belt comprising thin-bedded metachert (metamorphosed chert), slate and massive chert in the Paleozoic (Chichibu) system, and form a zone which trends N. 20°～30° E. and dips 45°～70° to the east. The Paleozoic sediments are penetrated by the Kobugahara and Sôri granodiorite intrusives probably of the Mesozoic age, and are weakly metamorphosed into hornfelses, the slaty rocks spotted by biotite being found in the vicinity of the mine.

The Odaki ore body, in which the pyrosmalite occurs, has been exploited since August, 1956, after the new concession of Odaki was amalgamated to the old Kyurazawa mining area. It belongs to the Kyurazawa manganese-ore zone, and is of tabular shape parallel to the general bedding of the country rocks. The Odaki ore body is about 1.5 m. in average width and has been developed along its strike for more than thirty metres.

The ore consists essentially of primary manganese-iron silicate minerals and contains 23～25 per cent. manganese and 23～25 per cent. iron in bulk. It has been utilized for metallurgical purposes in spite of its relatively high content of silica. The ore of higher grade occurs usually in the central part of the ore body bordered by fine-grained, banded rhodonite-spessartite ore.

The pyrosmalite, which is one of the important ore mineral in this mine, occurs as coarse granular aggregates with knebelite, spessartite, pyroxmangite, some other manganese silicate minerals and some sulphide minerals such as sphalerite, pyrrhotite, etc. as shown in Plate I, Fig. 1. Under the microscope it is often observed that anhydrous manganese silicate such as knebelite and rhodonite are re-

* 栃木県上都賀郡足尾町久良沢鉱山

placed by pyrosmalite. Remnants of knebelite are sometimes enclosed in platy crystals of pyrosmalite as shown in Plate II, Fig. 4. Fine grains of knebelite are also enclosed in the central cores of zoned pyrosmalite as shown in Plate II, Fig. 3.

Green chloritic minerals are also commonly found in the pyrosmalite-bearing manganese-iron ore (Plate I, Fig. 2).

Judging from the common association of pyrosmalite with iron-rich sphalerite and pyrrhotite, it is inferable that the sulphide mineralization took place intimately following the stage of hydration and chlorination of manganese silicates.

The writers consider that the coarse aggregates of pyrosmalite and knebelite have been formed in the manganiferous beds by pyrometasomatism in connection with the granodiorite intrusion. The banded rhodonite-spessartite rocks are, however, considered to be the recrystallization products due to thermal metamorphism of syngenetic manganiferous sediments.

Crystal habit

The tabular or prismatic crystals up to 3 cm. across are often found in vugs in the coarse aggregate of pyrosmalite and knebelite. The crystals are very simple in form and consist usually of the basal pinacoid in combination with hexagonal prism $\{10\bar{1}0\}$. The blocky texture as mentioned by Stillwell and McAndrew[3] is very common. The larger crystals commonly show distinct zonal structure, their central core being darker in colour owing to the presence of abundant inclusions of knebelite.

Physical and chemical properties

The mineral is transluscent and pale brown to brown in colour. Its fracture is uneven and splintery. Specific gravity is 3.14. Hardness is $4\frac{1}{2}$. The following optical properties have been determined:

$\omega=1.671$, $\varepsilon=1.639$, $\varepsilon-\omega=0.032$;

uniaxial and optically negative.

After decomposing the pyrosmalite by nitric acid, the presence of chlorine was tested by using $AgNO_3$ solution. Although the complete chemical analysis of the pure material has not been made, the presence of iron and manganese with a small amount of zinc was proved by X-ray spectrochemical analysis.

X-ray determination of pyrosmalite and knebelite

Carefully selected specimens of pyrosmalite and knebelite were examined by Philips Geiger counter X-ray diffractometer. The X-ray powder pattern of the pyrosmalite was compared with that of Broken Hill[3] and indexed in terms of a hexagonal cell as in Table 1. The lattice dimensions of the pyrosmalite from Kyurazawa were calculated from the d values of $(44\bar{8}0)$ for a_0 and of (0005) for c_0 as follows:

$$a_0=13.40\text{Å.}, \qquad c_0=7.135\text{Å..}$$

Table 1. X-ray powder data for the pyrosmalite from the Kyurazawa mine, Tochigi prefecture and that from Broken Hill mine, New South Wales.

Broken Hill[3]		Kyurazawa*				*hkil*
d (Å)	I	d (Å)	I	Q_{obs}	Q_{cal}	
11.5	20	11.65	1	0.0074	0.0074	$10\bar{1}0$
7.16	80	7.146	100	0.0196	0.0196	0001
6.65	5					$11\bar{2}0$
6.06	30	6.097	2	0.0269	0.0270	$10\bar{1}1$
5.74	5					$20\bar{2}0$
4.87	20					$11\bar{2}1$
4.50	10	4.501	1	0.0494	0.0493	$20\bar{2}1$
4.35	20	4.376	½	0.0522	0.0522	$21\bar{3}0$
3.73	20	3.740	½	0.0715	0.0716	$21\bar{3}1$
3.58	50	3.570	50	0.0784	0.0786	0002
3.41	40	3.411	3	0.0859	0.0860 0.0864	$10\bar{1}2$ $30\bar{3}1$
3.34	5					$22\bar{4}0$
3.15	tr.					$11\bar{2}2$
3.03	20					$20\bar{2}2$ $22\bar{4}1$

Table 1.—*Continued*

2.89	10					$40\bar{1}0$
2.77	10					$21\bar{3}2$
2.69	100	2.686	10	0.1386	0.1386	$40\bar{4}1$
2.61	tr.	2.622	½	0.1454	0.1454	$30\bar{3}2$
2.52	5					$41\bar{5}0$
2.38	10	2.328	1	0.1768	0.1768 0.1751 0.1755	0003 $31\bar{4}2$ $41\bar{5}1$
2.25	70	2.250	5	0.1975	0.1974 0.1991	$40\bar{4}2$ $11\bar{2}3$
2.20	tr.					$20\bar{2}3$ $50\bar{5}1$ $42\bar{6}0$
2.13	tr.					$32\bar{5}2$ $33\bar{6}1$
2.09	5					$21\bar{3}3$ $42\bar{6}1$ $51\bar{6}0$
2.02	tr.					$30\bar{3}3$
1.930	tr.					$60\bar{6}0$
1.912	tr.					$31\bar{4}3$
1.892	tr.					$33\bar{6}2$
1.840	50	1.839	2	0.2955	0.2956 0.2945	$40\bar{4}3$ $43\bar{7}1$
1.797	tr.					$51\bar{6}2$ $52\bar{7}1$
1.766	5					$10\bar{1}4$ $61\bar{7}0$
1.734	tr.					$41\bar{5}3$ $11\bar{2}4$
1.672	50	1.675	1	0.3564	0.3564	$44\bar{8}0$
1.629	40	1.6304	1	0.3762	0.3760 0.3773	$44\bar{8}1$ $33\bar{6}3$
1.608	tr.					$53\bar{8}1$ $70\bar{7}1$
1.588	tr.					$61\bar{7}2$
1.566	tr.					$51\bar{6}3$ $62\bar{8}1$ $31\bar{4}4$
1.521	50	1.5195	2	0.4331	0.4331	$40\bar{4}4$
1.459	5br.					$62\bar{8}2$ $52\bar{7}3$ $41\bar{5}4$ $63\bar{1}0$

Table 1.—*Continued*

1.427	tr.	1.4270	2	0.4912	0.4912 0.4874	0005 6391
$a_0=13.36$ Å $c_0=7.16$		$a_0=13.40$ Å $c_0=7.135$				

* unfiltered Fe radiation, slit: 1−0.006″−1, scanning speed: 1°/2 min., scale factor: 8, multiplier: 1, time constant: 8 sec.,

The abnormally strong reflection from the basal spacings are undoubtedly due to preferred orientation.

The X-ray powder data for the associated knebelite together with that from Dannemora are given in Table 2.

Table 2. X-ray powder data for the knebelite from Kyurazawa mine, Tochigi prefecture and that from Dannemora, Sweden.

Kyurazawa*		Dannemora*		
d (Å)	*I*	*d* (Å)	*I*	*hkl*
5.31	30	5.31	30	020
4.02	20	4.03	10	021
3.58	30	3.59	30	111
3.08	20	3.08	10	002
2.86	100	2.85	100	130
2.66	10	2.66	20	022
2.59	30	2.59	50	131
2.53	80	2.52	60	112
2.44	20	2.43	10	200
2.34	20	2.33	20	122
2.09	10	2.10	10	132
1.945	10	1.942	10	150
1.792	30	1.793	30	222
1.719	10	1.721	10	141
1.696	10	1.698	20	061
1.667	20	1.667	20	133
1.540	20	1.540	20	004
1.530	10	1.532	10	062

Table 2.—*Continued*

indexed by using		
a_0= 4.86 Å	a_0= 4.86 Å	(calculated from (222))
b_0=10.58	b_0=10.59	(〃 (062))
c_0= 6.16	c_0= 6.16	(〃 (004))

* unfiltered Fe radiation, slit: 1—0.006″—1, scanning speed: 2°/1 min., scale factor: 4, multiplier: 1, time constant: 4 sec..

Acknowledgements

The writers wish to thank Mr. B. Gokan for supplying the specimens from Kyurazawa. Their thanks are also due te Mr. T. Ando of the Hayashi Mining Company and Messrs. T. Osuga and Y. Kasahara of the Furukawa Mining Company for their kind assistance in the field. Further, the writers wish to acknowledge a grant from the Government Expenditure for Scientific Research.

References

1) Frondel, C. and L. H. Bauer: Amer. Miner., **38**, 755 (1953).
2) Hutton, C. O.: Amer. Miner., **41**, 51 (1956).
3) Stillwell, F. L. and J. McAndrew: Miner. Mag., **31**, 371 (1957).
4) Watanabe, T., et al.: Geological map of the Ashio Mountain District and its explanatory; Publication from the Tochigi Prefecture Office (1957).

Manuscript received November 29, 1957.

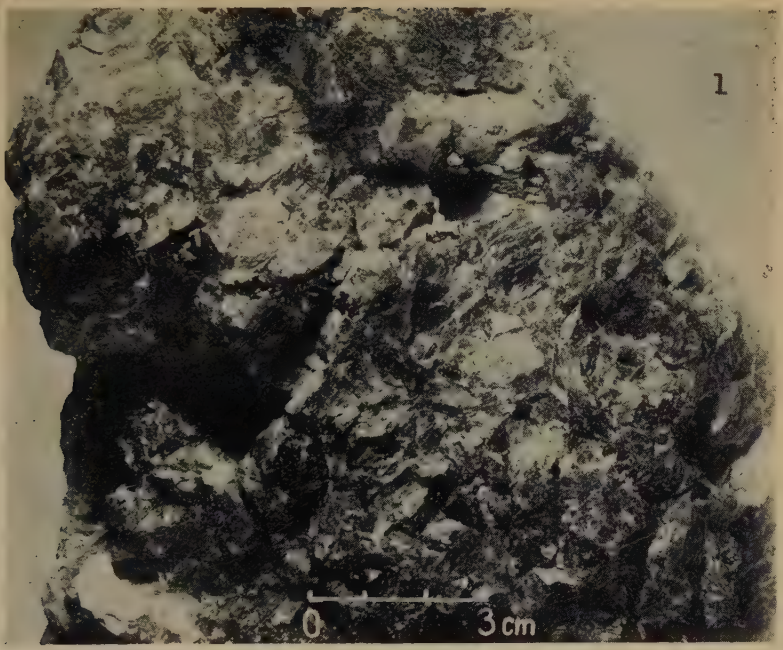

Fig. 1. Coarse aggregates of pyrosmalite with vugs in which cluster of its crystals are found.

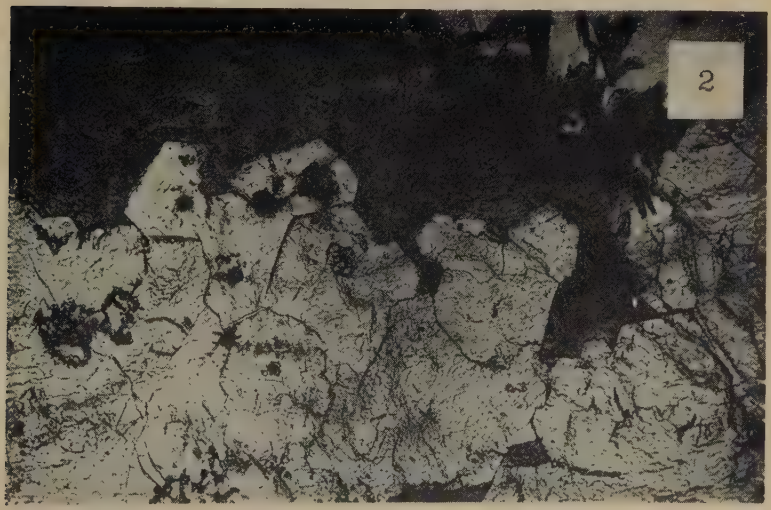

Fig. 2. Pyrosmalite crystals showing hexagonal outlines; interstitial space is filled with chlorite and quartz. (×70)

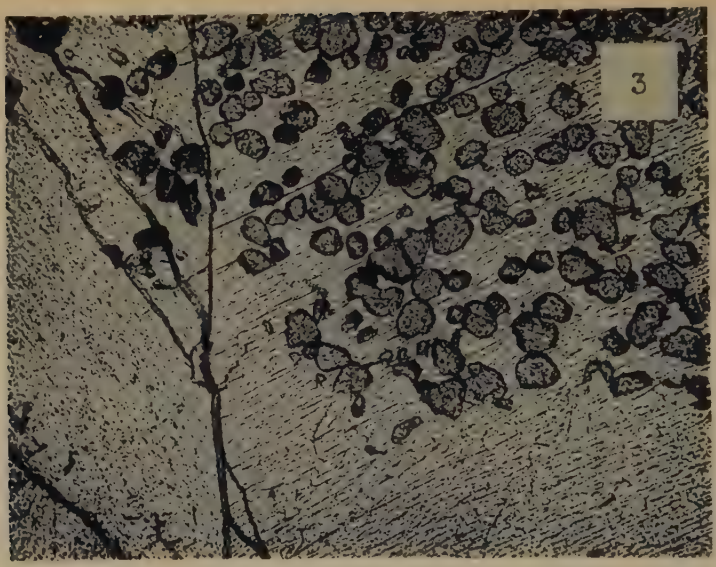

Fig. 3. A large zoned crystals of pyrosmalite with (0001) cleavage traces; euhedral and subhedral grains of knebelite are contained in their inner zone. (×70)

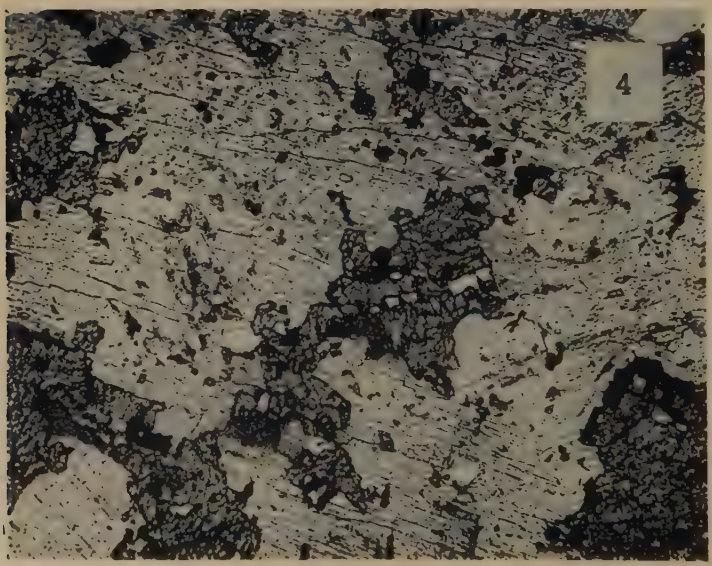

Fig. 4. A large crystal of pyrosmalite enclosing remnants of knebelite. (×70)

MINERALOGICAL JOURNAL, VOL. 2, NO. 3, PP. 187–192 DEC., 1957

SHORT COMMUNICATIONS

DIASPORE FOUND IN ASSOCIATION WITH ZINCBLENDE AND PYRITE ORES OF THE HANAOKA MINE, AKITA PREFECTURE

TOSHIO SUDO and HISATO HAYASHI

Geological and Mineralogical Institute, Faculty of Science, Tokyo University of Education

Introduction

In the course of the mineralogical study on wall rock alteration, the writers dealt with the altered area of the Tsutsumizawa ore deposit of the Hanaoka mine, Akita Prefecture. The Tsutsumizawa ore deposit is one of the principal ones of the mine, and is composed of many hydrothermal replacement ore bodies being worked by open cut. We can observe clearly the alteration halo developing around a group of the ore bodies in the central area of the open cutting. The ores are classified into the following types: black ore in zincblende and galena, yellow ore rich in pyrite and chalcopyrite, silicious ore and gypsum ore.

As the present writers have discussed previously,[4] the alteration zone can be classified into two: one is a narrow zone immediately in contact with ore bodies (B-zone), and the other developing around the B-zone (A-zone). The principal alteration product of the A-zone is montmorillonite and the product in the B-zone can be enumerated as chlorite (magnesium-rich chlorite) and sericite and rarely kaolin minerals. As far as data is concerned, sericite is dominant around yellow ore and silicious ore bodies, whereas chlorite is dominant around gypsum ore bodies. The mineral component of the altered

zone around the black ore bodies is very complex showing a close association of the minerals as sericite, chlorite, kaolin minerals, and also a clay mineral with the 30 Å. spacing.

The main scope of this short communication is to provide the latest noteworthy mineralogical data confirmed in the altered zone around a small black ore body in the Tsutsumizawa ore deposit.

Mineral association in the altered zone around a small black ore body

The mineral compositions of the several specimens collected from the altered zone around a small black ore body in the Tsutsumizawa ore deposit are as shown in Table 1. The identification of these minerals was based on X-ray and differential thermal analysis curves. The amount of these minerals was roughly and relatively estimated by comparing peak hights of thermal curves or X-ray powder reflections with one another.

Table 1. Mineral compositions of several specimens collected from the altered zone around a small black ore body in the Tsutsumizawa ore deposit.

Specimen	Kaolinite	Diaspore	Pyrite	Chlorite	Montmorillonite	30 Å-mineral
908	Med.	Much	Much	Med.	Med.	Much
410	Med.	Much	Much	Small	Neg.	Neg.
419	Med.	Much	Much	Neg.	Neg.	Small
543	Small	Neg.	Much	Small	Small	Small
316	?	Neg.	Med.	Much	Neg.	Neg.
411	Neg.	Small	Small	Much	Neg.	Small

Notes: Neg.: negligibly small, Med.: medium.

Thin section study revealed that diaspore and pyrite crystals are cemented by extremely fine clayey materials, which are the clay minerals listed in this Table.

The 30 Å. clay mineral, as the writers have reported previously[3)4)], is considered to be a regularly interstratified chlorite-montmorillonite clay mineral. X-ray study revealed that specimen 908 comprises the

30 Å. clay mineral as well as an irregularly interstratified montmorillonite-chlorite.

Since specimen 908 contains negligibly small amounts of iron and magnesium, the chlorite was identified as "aluminian chlorite".

Chlorite is dominant in specimens 543, 316 and 411. It is not certain whether these chlorites are also aluminian type or not, because their chemical analyses are not available. In the light of data to date, it has been suggested that chlorite found in close association with the black ore deposits usually belongs to a magnesium-rich member[1,2,4].

The presence of kaolinite was suggested by the fact that the 7 Å. and 3.5 Å. reflections occur with strong intensities in spite of the negligibly small amounts of magnesium and iron and the absence or very weak intensity of the 15 Å. reflection.

Mineral association in the black ore body

The ore is composed of zincblende and pyrite, accompanied by diaspore, barite and clayey materials.

Diaspore occurs as granular aggregates of short prismatic crystals sporadically spread over crystals of zincblende and pyrite. Its optical data are as follows: $\alpha=1.690\sim1.685$, $\gamma=1.737\sim1.730$, $\gamma-\alpha=0.047\sim0.045$ and $(+)2V=84°\sim86°$. These data agree fairly well with the earlier data for diaspore except that the refractive indices are slightly lower in the present case.

From the black ore, the writers separated and collected white minerals by elutriation as free from opaque minerals as possible. The X-ray powder diffraction data for these white minerals is as shown in Table 2. The powder reflections obtained revealed that this sample is mainly composed of diaspore and barite. But the writers would like to point out the following facts: (a) the 4.72 Å. reflection is stronger than what is expected in the case of diaspore, (b) the strong 2.36 Å. reflection, and the medium strong 1.573 Å. reflection are not attributed to diaspore, (c) the intensity of the 1.482 Å. reflection is stronger than that expected from the estimated content of diaspore

Table 2. X-ray powder diffraction data for white mineral powder separated from the black ore.

X-ray powder diffraction data for diaspore, brucite and barite are listed herein for reference.

White mineral powder		Diaspore*		Brucite*		Barite*	
d	*I*	*d*	*I*	*d*	*I*	*d*	*I*
4.72Å	60s	4.69Å	2	4.75Å	53		
4.40	5b					4.35Å	20
4.00	67s	3.98	10			3.89	25
3.58	5s	3.516	2			3.57	10
3.45	5s					3.44	63
3.33	4s					3.31	35
3.22	7s	3.216	2				
3.13	6s					3.10	63
2.86	2b					2.83	40
2.84	3s						
2.71	5b					2.72	45
2.60	3s						
2.56	25s	2.558	4				
2.50	2b					2.47	14
2.36	45b	2.36	1	2.35	100		
2.32	22s	2.312	8			2.31	10
2.22	4b					2.20	15
2.13	17s	2.124	7			2.10	100
2.08	48s	2.072	7			2.04	10
1.918	7s	1.892	1			1.92	5
1.873	2s					1.85	15
1.821	3b	1.807	1	1.79	40		
1.737	3b					1.74	8
1.713	3b	1.707	3				
1.684	2s					1.67	15
1.669	3s						
1.634	21s	1.603	2			1.63	8
1.610	9s						
1.573	10s			1.57	33	1.58	10
1.526	3s					1.52	25
1.482	11s	1.477	3	1.490	17		

Table 1.—*Continued*

1.448	2s						
1.432	5						
1.425	4	1.418	2			1.420	20
1.402	4s	1.397	1				
1.399	9s	1.372	3				

* After K. Kubo: Chemical Analyses by X-ray (1955).

in this specimen. It is strongly suggested that these facts may be attributed to the presence of brucite. The same facts were also noticed in the X-ray powder diffraction data for specimen 410. Although the presence of brucite was strongly suggested by X-rays, further studies, in addition to chemical analysis, are indispensable for its confirmation.

The differential thermal analysis curve of this white material is shown in Fig. 1. A strong endothermic peak occurs between 500°C.

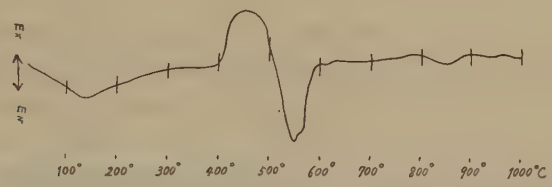

Fig. 1. Differential thermal analysis curve of the white mineral powder separated from the black ore of the Hanaoka mine.

and 600°C., which shows a sign of a double peak. One of the two branches of the peak may be attributed to diaspore.

Summary and consideration

In the light of the X-ray and thermal data obtained, the following mineral associations can be confirmed.

In the altered zone: Chlorite-montmorillonite-kaolinte-30 Å. clay mineral-diaspore-pyrite.

In the black ore body: Pyrite-zincblende-diaspore-barite-brucite(?).

The occurrence of such mineral associations have not been hitherto anticipated in black ore deposits. We are deeply interested in the research on the environmental condition forming such mineral association, but we have not yet reached a final conclusion. At present, we may give the following suggestion.

As far as the data is concerned, diaspore is liable to be in close association with kaolin minerals and not with montmorillonite or chlorite, and clay minerals such as chlorite, montmorillonite and kaolin minerals tend to be dominant in altered zones, whereas hydroxide minerals such as diaspore and brucite are liable to be dominant in ore bodies. Thus it seems to be natural to consider that the environmental condition in this ore body is more favourable for the formation of hydroxide minerals than that in the altered zone.

Acknowledgement

The writers are greatly indebted to Mr. Tatsuo Toraiwa of the Hanaoka mine for his helpful guidance with regard to geological observation, and to Mr. Shinji Sato of Tokyo University of Education for measurements of optical constants of diaspore. Thanks are also due to the officials of the Department of Education for their kind courtesy to grant fund for this study.

References

1) Iwao, S.: Jap. Journ. Geol. Geograph., **26**, 105 (1956).
2) Sakamoto, T. and T. Sudo: Miner. Jour., **1**, 348 (1956).
3) Sudo, T., H. Takahashi and H. Matsui: Jap. Journ. Geol. Geograph., **24**, 71 (1954); Nature, **173**, 261 (1954).
4) Sudo, T. and H. Hayashi: Sci. Reports Tokyo Kyoiku Daigaku (Tokyo Univ. of Education), C, No. 23, 173 (1955).

Manuscript received April 19, 1957.

MINERALOGICAL JOURNAL, VOL. 2, NO. 3, pp. 193-195, DEC., 1957

IRON-RICH SAPONITE FROM MAZÉ, NIIGATA PREFECTURE, JAPAN

NOBORU MIYAMOTO

Geological and Mineralogical Institute, Faculty of Science, Tokyo University of Education

Although some of the green minerals in altered andesite or basalt is expected to be iron-rich saponite[1], detailed mineralogical data to determine them have not yet been obtained owing to the difficulty of separation of the minerals. Recently, in the course of the study of zeolites from Mazé, Niigata Prefecture, the writer confirmed the widespread occurrence of green minerals in altered basalt and its tuff breccia, and was able to identify one of them as iron-rich saponite.

Iron-rich saponite from Mazé has dark green colour and occurs filling amygdales, or as alteration products of glassy material or plagioclase fragments in altered basalt or its tuff breccia. Thin section study revealed that it occurs usually as thin film covering the inner walls of the amygdales which are filled by zeolites or calcite (Fig. 1), and forms aggregates of extremely fine particles apparently iso-

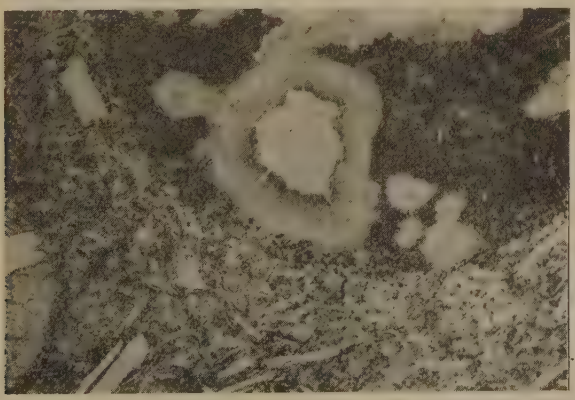

Fig. 1. Iron-rich saponite occurring as thin film covering the inner walls of amygdales. (×20)

tropic or of extremely fine fibrous crystals with refractive indices: 1.53~1.56, double refraction: 0.02~0.03.

The d.t.a. curve for the saponite recorded at the mean heating rate of 10°C. per minute is shown in Fig. 2. The curve shows a

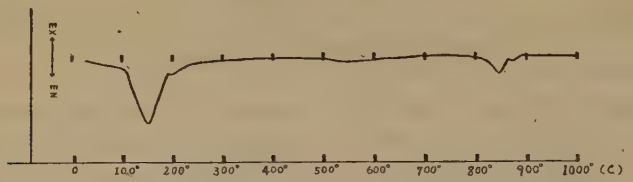

Fig. 2. d.t.a. curve for iron-rich saponite from Mazé.

sharp endothermic peak between 100° and 200°C., a small endothermic peak at about 200°C., a very weak and broad endothermic peak between 500° and 600°C., and a distinct double endothermic peak at about 850° and 870°C..

Table 1. X-ray powder diffraction data for the iron-rich saponite from Mazé. (Cu $K\alpha$ radiation)

hkl, *hk*	*d*(Å)	*I*
001	15.6±0.8	16s
11,02	4.56	7b
13,20	2.63	5vb
33,06	1.533	8s
E.G.	17.3±0.1	

Its X-ray pattern was recorded by X-ray diffractometer. It is composed of broad peaks as listed in Table 1. Treatment with ethylene glycol caused the 15.6±0.8Å. reflection to be replaced by the 17.3±0.1Å. reflection. ("E.G." in Table 1).

The chemical composition of the reference specimen free from impurities is as follows:

SiO_2 43.98, TiO_2 0.16, Al_2O_3 6.30, Fe_2O_3 7.85, FeO 5.32, MnO 0.32, CaO 2.78, MgO 18.02, $H_2O(+)$ 9.24, $H_2O(-)$ 6.24, total 100.39%.

From this chemical analysis, the following structural formula can be obtained:

$(Mg_{2.09}\ Fe^{++}_{0.35}\ Mn^{++}_{0.02}\ Fe^{3+}_{0.40})\ (Al_{0.58}\ Si_{3.42})O_{10}\ (OH)_2\ (Ca/2)_{0.46}$.

The data obtained thus far well agree with the properties of iron-rich saponite.

The writer wishes to offer his sincere thanks to Professor T.

Sudo of the Geological and Mineralogical Institute, Tokyo University of Education for his kind guidance during the present work.

REFERENCES

1) T. Sudo: Journ. Geol. Soc. Japan, 60, 18 (1954).

Manuscript received September 15, 1957.

MINERALOGICAL JOURNAL, VOL. 2, NO. 3, PP. 196-199, DEC., 1957

ZEOLITE-BEARING BENTONITES

HISATO HAYASHI and TOSHIO SUDO

Geological and Mineralogical Institute, Faculty of Science,
Tokyo University of Education

The occurrence of zeolite in bentonite has been reported by Bramlette and Posnjak[1], Ross and Hendricks[4], and Sudo[5]. Recently, in the course of our mineralogical and geological studies on Japanese bentonites and so-called acid clays, we have found a considerable number of new localities of zeolite-bearing bentonites, and we have noticed that they are not so rare in Japan as we have hitherto believed. The purpose of this communication is to introduce the mineralogical and geological data of such bentonite as illustrated by two representative reference specimens (Yokoté clay, Akita Prefecture and Bodai clay, Ishikawa Prefecture).

Yokoté clay is found as bedded forms in tuff and tuffaceous sediments. Its macroscopic appearance is of the common clay such as porous sandy and/or compact clayey. Thin section study revealed that the original rock of this bentonite is porous pumice tuff, and pumice fragments with vesicular textures have altered to montmorillonite. The interstices of pumice fragments are filled by aggregates of the following materials: zeolite crystals, rounded opal grains and angular fragments of a transparent glassy material. Zeolite crystals show low double refraction, clear cleavage, and nearly parallel extinction; they rarely show prismatic crystal shapes. Angular fragments of a glassy material (Table 1 (3)) have a refractive index of 1.497 (16.5°C.) and it was confirmed by X-ray studies that they are nearly amorphous. The total amount of zeolite crystals, opaline silica and the transparent glassy material may make up as much as 30~50 per cent. of the rock.

Table 1. Chemical compositions of zeolite-bearing bentonites and related materials.

	Yokoté, Akita Prefecture			Bodai, Ishikawa Prefecture	
	(1)	(2)	(3)	(4)	(5)
SiO_2	72.37%	63.21%	67.82%	61.70%	66.96%
TiO_2				0.30	tr.
Al_2O_3	12.34	12.47	17.43	13.97	12.66
Fe_2O_3	2.79	1.23		2.12	0.82
FeO			1.18	0.14	
MnO				0.01	
MgO	2.76	1.07	1.06	0.74	0.80
CaO	1.78	2.50		2.78	5.96
Na_2O	1.34	1.77	3.11	3.46	2.94
K_2O	1.10	0.17		0.36	0.40
Ig. loss	6.39	18.17	7.54	5.30	6.28
H_2O (−)			2.60	9.48	2.96
Total	100.87%	100.59%	100.74%	100.36%	99.78%

(1) Sandy part dried at 100~110°C., (2) Clayey part dried at 100~110°C. (K. Yoshizaki, analyst). (3) Transparent angular fragments of a glassy material; the specimen was collected by hand picking, and clayey materials were removed perfectly by washing with water (A. Hayashi, analyst). (4) Clayey part (H. Hayashi, analyst). (5) Zeolite of the mordenite group; aggregates of crystals like fine silk threads (H. Hayashi, analyst).

Bodai clay is found in the boundary zone between tuff and liparite; perlite frequently accompanies the latter (Table 1 (4)). Further away from the boundary zone, the alteration becomes less intense and clayey rocks gradually grade into fresh ones. Near the boundary zone, both tuff and liparite are found as the original rocks of this bentonite. It is worthy of notice that the amount of zeolite is usually negligible in the bentonite of tuff-side, whereas it is clearly confirmed in that of liparite-side. Furthermore, nodules (1 mm. in mean size) of opaline silica and/or aggregates (2 cm. in mean size) of zeolite crystals like fine silk threads surrounded by opaline silica are sporadically patched in the bentonite of liparite-side (Table 1 (5)).

X-ray studies revealed that X-ray powder reflections of these bentonites are attributed to montmorillonite, cristobalite due to opaline silica, and also to a zeolite of the mordenite group (Table 2 (1)).

Table 2. X-ray powder diffraction data for zeolite-bearing bentonite and zeolite crystal aggregates.

(1)				(2)					
Zeolite-bearing bentonite Yokoté, Akita Prefecture				Zeolite crystal aggregates Bodai, Ishikawa Prefecture					
d	*I*	*d*	*I*	*d*	*I*	*d*	*I*	*d*	*I*
16.1Å	20b	2.98Å	7s	13.8Å	38s	3.49Å	38s	1.998Å	13s
9.1	10s	2.89	3b	9.2	221s	3.41	130s	1.957	17s
8.0	4b	2.81	3s	6.6	43s	3.21	144s	1.888	8s
6.7	6b	2.58	7b	6.42	35s	3.12	14b	1.814	31s
5.79	4vb	2.53	8b	6.11	18b	2.90	42s	1.797	10s
5.34	4vb	2.46	5b	5.83	83s	2.71	13s	1.725	4vb
5.16	4b	2.036	3s	5.09	7vb	2.64	8vb	1.700	10s
4.51	17s	1.884	3b	4.87	6vb	2.57	23s	1.667	9s
4.10	22b	1.695	3b	4.55	140s	2.54	21s	1.623	5vb
4.00	23s	1.501	5s	4.17	41s	2.47	17s	1.600	7b
3.48	13s	1.455	3s	4.02	136s	2.44	10vb	1.551	10s
3.40	9s			3.87	26s	2.28	8vb	1.530	15s
3.23	11s			3.77	12b	2.23	9s	1.484	8s
3.19	8s			3.65	12b	2.14	5vb		
3.13	6s			3.59	20s	2.049	15s		

s: sharp, b: broad, vb: very broad.

Furthermore, in the light of the X-ray and chemical data, zeolite found as aggregates of crystals like fine silk threads well agrees with that of the mordenite group (the ptilolite-mordenite series) including silica-rich zeolites in the light of earlier data (Koizumi and Kiriyama[3], Harris and Brindley[2], (Table 2 (2)). It is noticed that some principal powder reflections of montmorillonite, opaline silica (cristobalite) and the zeolite overlap with one another. The 14~16 Å. reflection is attributed to montmorillonite or zeolite, the 4 Å. reflection is attributed to zeolite or opaline silica (cristobalite). The 9 Å. and 6 Å.

reflections are the key to suggest the presence of zeolite.

Generally speaking, the mode of occurrence of zeolite-bearing bentonites from other localities is of the similar type as that of Bodai material. As far as data to date concerned, it is considered that hydrothermal or hot spring actions played an important role in forming these zeolite-bearing bentonites.

As one of the problems concerning the utilization of zeolite-bearing bentonite, the writers are comparing the efficiency of its adsorptive power with that of the usual bentonite.

REFERENCES

1) Bramlette, M. N. and E. Posnjak: Amer. Miner., **18**, 167 (1933).
2) Harris, P. G. and G. W. Brindley: Amer. Miner., **39**, 819 (1954).
3) Koizumi, M. and R. Kiriyama: Sci. Rep. North College, Osaka Univ., No. 2, 67 (1953).
4) Ross, C. S. and S. B. Hendricks: U. S. Geol. Surv. Prof. Paper., 205-B, 23 (1945).
5) Sudo, T.: Journ. Geol. Soc. Japan, **56**, 13 (1949).

Manuscript received November 7, 1957.

ABSTRACT OF THE KOBUTSUGAKU ZASSHI,

JOURNAL OF THE MINERALOGICAL SOCIETY OF JAPAN, VOL. 3, NO. 3,

June, 1957

Studies on the Impurity of Synthetic Corundum (pp. 187-208)

Takuya Imai

Synthetic corundum and its raw materials were chemically analysed with special reference to impurities and the results obtained were discussed from the mineralogical point of view. The crystal structure of raw alumina may be of αAl_2O_3, γAl_2O_3, or their mixture, and none of the impurities gives rise to modification of the structure. Boule is not a single crystal identical with the native corundum, but may be regarded as "monocrystal" composed of single crystals slightly shifted from each other.

Among colouring materials for various corundums, chromium oxide for synthetic ruby was investigated in detail. The unit cell dimension a_0 of synthetic ruby increases with the content of Cr_2O_3, which also affects the tone of colour, specific gravity, refractive indices and the angle between the c-axis and the growing axis of boule. The data obtained imply that the Cr atoms in synthetic ruby are distributed homogeneously throughout boule replacing Al atoms.

Chlorite in the So-Called Propylite of the Yugashima Mine (pp. 209-213)

Takayo Fujiwara

The mineralogical properties of the chlorite in propylite of the Yugashima series in the Yugashima mine are given, i. e. optical character, chemical constitution and X-ray powder lines. As the result, the chlorite's structural formula was determined as $(Mg_{2\cdot6}\ Fe^{++}_{1.4}\ Fe^{+++}_{0.4}\ Al_{0\cdot8})\ (Si_{\ 2\cdot6}\ Al_{\ 1\cdot4})O_{10}\ (OH)_8$, which is inferred to belong in ripidolite.

Autunite from the Ningyô Pass on the Boundary between Tottori and Okayama Prefectures, Japan (pp. 214-217)

Tokuzo Soma

Autunite from the Ningyô pass occurs disseminated through the conglomerate and sandstone of the upper Tertiary uranium bearing lacustrine beds, which rest on a peneplainated mass of biotite granite. The optical, X-ray and chemical properties of the autunite are described in this paper. The uranium-radium ratio of the mineral indicates its age to be about thirty six thousand years.

On the Heat of Hydration of Ions (pp. 218-227)

Masaru Goto and Shunji Matsuda

Goto, in his previous report on the solubility of ionic salts, presumed that the water molecules combine with negative ions in the same manner as with positive ions, their dipole moment and the center of the ions lying on a straight line. According to this model, the writers calculated the heat of hydration, U_h, of alkali and halogen ions by the following equation,

$$U_h = n \cdot \beta \cdot z \cdot e \cdot \mu/(r+L)^2 + m \cdot z \cdot e \cdot \mu/(r+2r_w+L)^2 + \frac{z^2e^2}{2(r+4r_w+L)}\left(1-\frac{1}{\varepsilon}\right) - U_w,$$

where n: number of water molecules in contact with an ion; probably equal to 4 for all alkali and halogen ions,

m: those in the second layer of the hydration sphere,

β: crystallodinamic constant after Bernal,

z: ionic valency, e: elementary charge,

μ: dipole moment of water molecule,

r: radius of ion, r_w: radius of water molecule,

L: effective radius of water molecule; $(r_w+0.25)$Å. for positive ions and $(r_w-0.25)$Å. for negative ones,

ε: dielectric contsant of water,

U_w: heat consumed for destruction of the structure of water due to the coordination of water molecules to ions.

By applying a graphical method, the values of m, β and U_w were determined to be 90, 0.9 and 30 kcal/g. ion respectively. Hence, the values of the

heat of hydration of alkali and halogen ions were obtained as follows: Li^+ 125.8, Na^+100.7, K^+79.5, Rb^+71.8, Cs^+65.0, F^-112.2, Cl^-80.5, Br^-73.1 and I^-63.1 kcal/g. ion.

Short Communications

On the Ninelings of Cassiterite from Naégi, Gifu Prefecture (pp. 228-233)

Fumiyuki Marumo

The ninelings of cassiterite from the Ebisu mine and the placer deposits in the Naégi district were measured by use of a two-circle goniometer. The idealized form of them is composed of a host crystal and eight individuals each at twinning position after $e\{011\}$ with the host. The twin may have originated at an early stage of crystal growth, it is implied by the feature of zonal structure in the nineling.

Powellite from the Kokurobé Mine, Toyama Prefecture (pp. 234-235)

Kitinosuke Henmi and Hisao Otsuka

Powellite with light green colour and light yellow fluorescence have been found in the molybdenum mine of Kokurobé, Toyama Prefecture, Japan. It occurs as an earthy pseudomorph after molybdenite. Its chemical composition is as follows: SiO_2 0.1, MoO_3 69.7, WO_3 1.5, FeO 1.2, CaO 26.0, MgO 1.0, ignition loss 0.9, total 100.4%. Its X-ray powder pattern was compared with those of scheelite and artificial $CaMoO_4$.

Communications on Minerals of Japan (Part 10) (pp. 236-243)

Mumeikai Group

22. *Uraninite from Nagatejima, Ishikawa Prefecture*

Kin-ichi Sakurai and Akira Kato

Uraninite crystals of cubic habit were found in a pegmatite of Nagatejima, accompanied by other radioactive minerals.

23. *Uraninite from Fusamata, Tochimoto and Shiozawa, Fukushima Prefecture*

Otokichi Nagashima, Kin-ichi Sakurai and Akira Kato

Three new localities of uraninite have been found in the Abukuma moun-

tain land. As in the localities previously known in this region, uraninite occurs embedded in plagioclases adjacent to lepidomalane in pegmatite. At Fusamata it accompanies fergusonite, while at Tochimoto and Shiozawa, it is usually surrounded by autunite.

24. *β-Uranophane from Tochimoto, Fukushima Prefecture*

Otokichi Nagashima and Akira Kato

Light yellow acicular crystals collected from the pegmatite of Tochimoto have been determined as β-uranophane in the light of its X-ray powder pattern as well as its optical characters.

25. *A Mineral Resembling Todorokite Found in the Ikeshiro Mine, Shizuoka Prefecture*

Kin-ichi Sakurai and Shin'ichiro Takasu

A brownish black fibrous manganese ore from the Ikeshiro mine was found out to have similar chemical composition and crystal structure as todorokite.

Reviews

The Measurement of the Intensities of Diffraction by X-Ray Diffractometer ..... Yoichi Iitaka 244-264

Proceedings 265-271

ABSTRACT OF THE KOBUTSUGAKU ZASSHI,

JOURNAL OF THE MINERALOGICAL SOCIETY OF JAPAN, VOL. 3, NO. 4,

October, 1957

Addresses

New Techniques in X-Ray Crystallography Involving the Use of Anomalous Dispersion (pp. 273-285)

Yoshihiko Saito

Two techniques in X-ray structure determination involving the use of anomalous dispersion have been reviewed; namely, Bijvoet's absorption edge technique for the determination of absolute configuration of optically active crystals and the method of P_s function of Okaya, Saito and Pepinsky for solving noncentrosymmetric structures. The intensities from the planes (hkl) and $(\bar{h}\bar{k}\bar{l})$ in noncentrosymmetric crystals are no more equal when anomalous scattering occurs. This fact is illustrated, zincblend being taken as an example. The results of the determination of absolute configuration hitherto performed are summarized and the methods employed for the comparison of (hkl) and $(\bar{h}\bar{k}\bar{l})$ intensities are described and criticized. Importance of the knowledge about the absolute structure and absolute configuration in stereochemistry, mineralogy and other fields is emphasized.

The principle of the method of P_s function is described. P_s is defined as follows:

$$P_s(u, v, w) = \sum_{hkl} |F(hkl)|^2 \sin 2\pi(hu+kv+lw).$$

It can be evaluated directly from the observed intensities. It is shown that P_s establishes the sense of the noncentrosymmetric distribution of nonanomalous scatterers about an anomalous scatterer. Thus P_s function provides significant assistance in solution of the phase problem. Moreover, it enables one to establish the absolute structure straightforwardly without any previous knowledge about the crystal structure. A few examples of the application of this method are included.

The Discovery of Mixed-Layer Minerals and Its Contributions to Clay Sciences (pp. 286-299)

Toshio Sudo

Recent advance of clay mineralogy particularly concerns with the discovery of mixed-layer minerals with various types. Its advance has revealed that properties of a clay mineral are, in some cases, more at variance than we have hitherto anticipated, that is, we have noticed some clay minerals being akin to both of two kinds of clay minerals. Those particular kinds of clay minerals can be regarded as "intermediate species" and classified into "mixed-layer type" and "distortion type".

Taking into consideration the crystallographical, mineralogical and geological knowledges thus far obtained, the writer has introduced an idea about the system of classification of clay minerals. In this system, "intermediate species" seem to play an important role to indicate the trend of field of clay minerals.

Original Articles

Studies on Manganese-Wads from some Localities in Hokkaido (pp. 300-313)

Yu Hariya and Zyunpéi Harada

Manganese-wads from some localities in Hokkaido were studied by chemical analysis, differential thermal analysis, X-ray diffraction and electron microscopy.

Differential thermal analysis curve of the manganese-wad from the Komagadaké mine does not show any distinct thermal reaction between endothermic peaks at about 150°C. and 650°~670°C.. The manganese-wad from the Akan mine exhibits endothermic peaks at 150°~180°C. and 640°~670°C., while that from Niimi Hot Spring, very distinct endothermic peaks at 665°C. and 1010°C..

The results of the X-ray powder method reveals that those wads are the mixture of some manganese oxide minerals, such as pyrolusite, cryptomelane, ranciéite and birnessite. Under the electron microscope they consist of fibrous aggregate, tabular crystal or amorphous matrix. They have been probably deposited from manganous mineral spring water by air-oxidation on the surface of the earth.

Boehmite in "Rôseki" (pp. 314-321)

Zyunpéi Harada and Takeshi Mitsuda

The writers found boehmite in 'Rôseki", agalmatolite, occurring as hydrothermal alteration product of liparite at Mitsuishi in western Japan. The results of X-ray, thermal and microscopic studies are summarized as follows:

The boehmite from Mitsuishi is of fine granular aggregate accompanied by pyrophyllite, kaolinite and diaspore. Its X-ray diffraction pattern agrees closely with that of synthetic boehmite investigated by P. P Reichertz and W. J. Yost. After heating, air-quenched samples are examined by X-ray. The diffraction pattern persists up to 450°C., but the characteristic peaks of boehmite disappears completely above 600°C..

Short Communications

Boehmite in Some "Rôseki" Deposits (pp. 322-325)

Taro Ota and Tsutomu Yamamoto

The occurrence of boehmite in "Rôseki" deposits of the Oohira mine in Mitsuishi Town, Okayama Prefecture and of the Ebara mine in Hidaka Town, Hyôgo Prefecture has been revealed by the writers. At the Mitsuishi mine, boehmite occurs in high alumina area as spherical or irregular nodules about 1 cm. across mixed with kaolin minerals and pyrophyllite. At the Ebara mine, boehmite rich nodules are disseminated in kaolin and the spherical nuclei of the nodules 3~5 mm. across are mainly composed of pure boehmite accompanied by only a small amount of kaolin minerals and diaspore as revealed by X-ray powder photographs and the following chemical composition: SiO_2 2.95, TiO_2 0.04, Al_2O_3 80.60, Fe_2O_3 0.72, CaO 0.14, MgO 0.02, ign. loss 15.67, total 100.14%.

X-Ray Diffraction Study of Silicified Wood (pp. 326-328)

Shiro Kanematsu

The constituent minerals of three specimens of silicified wood collected from the Plio-Pleistocene Kobiwako formation were identified by use of a Norelco X-ray refractometer. The main constituents are low quartz, and in addition

amesite, pyrite and magnetite are detected in a perfectly silicified specimen, while it is difficult to determine the constituents other than low quartz in poorly silicified one with considerable amount of carbon. The crystallization stage of the amesite may be inferred later than silicification, but further investigation is indispensable.

The Communications on Minerals of Japan (Part 11)

(pp. 329-337)

Mumeikai Group

26. *Pyrite from Yanahara Mine, Okayama Prefecture*

Nagashi Ogushi

Idiomorphic crystals of pyrite 1.5~2 cm. across have been found embedded in massive pyrrhotite surrounding the pyrite ore bodies of Yanahara Mine. Observed forms are $a\{100\}$, $o\{111\}$, $n\{211\}$, $m\{311\}$ with small $e\{210\}$. The interstices between pyrite crystal and pyrrhotite are usually filled with thin films of chalcopyrite.

27. *Manganite from the Oyé Mine, Niigata Prefecture*

Shin'ichiro Takasu

Manganite from the Oyé mine occurs as hard concretion 1~5 cm. across in pink clay. The concretion is an aggregate of munite euhedral or subhedral crystals whose pyramidal faces are observed on the surface of the concretion. Chemical analysis by H. Nagashima gave following results: MnO 72.63, O 9.08, SiO_2 3.50, Al_2O_3 tr., Fe_2O_3 0.22, CaO 0.04, MgO tr., BaO 1.33, $H_2O(+)$ 12.92, $H_2O(-)$ 0.32, total 100.04%. The X-ray powder pattern well agrees with previous data.

28. *Abukumalite from Suishoyama, Fukushima Prefecture*

Kin-ichi Sakurai

Short hexagonal prismatic crystals of Abukumalite attaining up to 13 mm

in diameter were collected from the pegmatite of Suishoyama. The surface of the crystals is dark bluish grey colour, but the interior is composed of greyish white earthy material with remnants of abukumalite of dark reddish brown colour and resinous luster. The X-ray powder pattern of the reddish brown part agrees well with that of the typical abukumalite, while the pattern of the white earthy part implies its decomposition products

29 *β-Uranophane from Yamanoo, Ibaragi Prefecture*

Akira Kato

A lemon yellow crust collected from the pegmatite of Yamanoo has been identified as β-uranophane by X-ray powder diffractions

Reviews

Fluorescent X-Ray Spectrographic Method.....
.....Zyunpéi Harada, Yu Hariya and Tadao Nagai...338-357

Proceedings 361-367

Mineralogical Society of Japan

OFFICERS FOR 1957–1958

President: Teiichi Ito, University of Tokyo, Tokyo.

Vice-President: Bumpei Yoshiki, Asahi Glass Co. Ltd., Tokyo.

Secretary: Toshio Sudo, Tokyo University of Education, Tokyo. Keiichi Omori, Tohoku University, Sendai.

Treasurer: Tokugoro Shoda, University of Tokyo, Tokyo.

Editor: Nobuo Katayama, University of Tokyo, Tokyo.

Councillors: Zyunpéi Harada; Hokkaido University, Sapporo. Keiichi Omori, Tsunehiko Takeuchi; Tohoku University, Sendai. Teiichi Ito, Shuichi Iwao, Nobuo Katayama, Eiichi Minami, Ryoichi Sadanaga, Tokugoro Shoda, Seitaro Tsuboi, Takeo Watanabe; University of Tokyo, Tokyo. Toshio Sudo, Tokyo University of Education, Tokyo. Teiroku Sueno, Onoda Cement Co. Ltd., Tokyo. Ichiro Sunagawa, Geological Survey of Japan, Tokyo. Kin-ichi Sakurai, Tokyo. Ryoiti Kiriyama, University of Osaka, Osaka. Kitinosuke Henmi, Okayama University, Okayama. Yoshio Kinosaki, Hiroshima University, Hiroshima. Kameki Kinoshita, Toyofumi Yoshimura; Kyushu University, Fukuoka.

PUBLICATIONS

Kôbutsugaku Zasshi, Journal of the Mineralogical Society of Japan

A journal containing articles and reviews on mineralogy and allied sciences contributed by members of the Mineralogical Society of Japan. Published every four months, in Japanese. Sent to all members of the Society. Membership dues $2.00 annually.

Mineralogical Journal

A journal containing articles on mineralogy and allied sciences, published semi-annually in English principally. Contributions are invited from everyone. The Journal completed its first volume of six numbers in 1956. Back numbers may be obtained at $1.00 per single copy for the time being. The price of subscription to the second volume is $5.00 per volume.

Printed by "HERALD" Printing Co., Ltd.